ADVANCED REGISTRATION TOOLS FOR XFM

by

F. Aytaç Durmaz

BSc, Electrical and Electronics Engineering, Bilkent University , 2007

Submitted to the Institute of Biomedical Engineering
in partial fulfillment of the requirements
for the degree of
Master of Science
in
Biomedical Engineering

Boğaziçi University
2010

ADVANCED REGISTRATION TOOLS FOR XFM

APPROVED BY:

Assist. Prof. Dr. Cengizhan Öztürk .....
(Thesis Advisor)

Assoc. Prof. Dr. Alp Dinçer .....

Prof. Dr. Ahmet Ademoğlu .....

DATE OF APPROVAL: 02 February 2010

ACKNOWLEDGMENTS

I would like to thank all people who have helped and inspired me during my doctoral study.

I especially want to thank my advisor, Assoc. Prof. Dr. Cengizhan Öztürk, for his guidance during my research and study at Boğaziçi University. His perpetual energy and enthusiasm in research had motivated all his advisees, including me. He provides me constant encouragement and a perfect balance between guidance and freedom throughout this study.

I was delighted to be a part of BUMIL family. They made BUMIL a perfect place to work. I would like to thank especially XFM group; Merdim, Emre, Abdülkadir they have inspired and support me during my studies. I would like to thank Onur, Alper, and Esin for their friendship during long hours in the lab.

I am grateful to Dr. Robert Lederman, and Antony Z. Faranesh at NHLBI, for their support and belief on this thesis.

I would like to appreciate The Scientific and Technological Research Council of Turkey for supporting XFM project under Grant number EEEAG-107E274.

My deepest gratitude goes to my family for their unflagging love and support throughout my life; this thesis is simply impossible without them. I am indebted to my mother, for his care and love. Thanks to my father for his guidance and visions that he shared with me through his life. I feel proud of my sister, Hande, for her talents. I believe she will be very happy, and my brother for being there with me when I need. Last but not least, thanks to Meltem for to be here through my life through these tests and challenges. You have made my life more eloquent.

ABSTRACT

ADVANCED REGISTRATION TOOLS FOR XFM

Minimally invasive therapies are very common in today's healthcare. Many procedures which require invasive surgery, with its associated long recovery times and high cost, can now be performed more effectively, with less trauma to the patient, by using smaller incisions and specialized surgical instruments. During interventional studies X-ray Angiography provides us with high resolution images at sufficient frame rate, but it doesn't have the desired soft tissue contrast. MR imaging on the other hand provide 3-D anatomic imaging with excellent soft tissue contrast.

Our aim is to fuse 2-D X-ray images with a priori 3-D MR volumes during medical interventions to assist physicians. X-ray fused with MRI (XFM) is an approach which combines strengths of both image modalities to improve the quality of image-guidance during minimally invasive interventions. In XFM, pre-operative MR images are segmented, 3D structure of target area is reconstructed from these segments, and after registration its projection is overlapped on top of live images during X-ray fluoroscopy.

Fusion of two modalities requires registration which could be achieved by using several algorithms. In this study we are using an intensity based 2D-3D registration algorithm rigid, multimodality intrasubject registration using mutual information between two modalities. The results of intensity based algorithm is compared with fiducial based registration results for the same datasets.

Our preliminary results show that our method has the potential to locate the MR image on top of 2D X-ray image with high accuracy in fusing both modalities.

Keywords: Image-Guided Medical Intervention, X-ray Fused with MRI (XFM), Intensity Based Image Registration, Hybrid (MRI X-ray) Imaging Systems.

XFM İÇİN YOĞUNLUK TABANLI ÇAKIŞTIRMA ALGORİTMASI

Girişimsel tedaviler günümüz sağlık dünyasında oldukça sık kullanılır hale gelmiştir. Kateter temelli operasyonlar düşük maliyet, çabuk iyileşme ve kolay operasyon süreci sağlamakta ve hasta için olan riskleri minimize etmektedir. Girişimsel temelli operasyonlarda X-ışınlı floroskopi şu anda altın standarttır. Cihazın gerçek zamanlı çalışması ve yüksek zamansal ve boyutsal çözünürlük operasyonlar için gerçek bir avantaj oluşturmaktadır. MR görüntüleme ise X-ışınlı cihazlarda elde edilemeyen yumuşak doku karşıtlığı ve 3 boyutlu anatomik görüntü sağlamaktadır.

Bu projedeki amacımız daha önce alınmış bulunan MR görüntülerini girişim sırasındaki görüntülerin üstüne çakıştırmaktır. Çakıştırma için bu farklı iki modalite arasında imge yoğunluklarından yararlanan bir algoritma kullanılmıştır. Girişimsel anjiyografide yumuşak dokuların görüntülenmesindeki yetersizlikler uygulamacılar için zorluk teşkil etmektedir. Bu sıkıntıyı aşmak için yumuşak doku karşıtlığı yüksek olan MR görüntülerinden faydalanılabilir. MR görüntülerinden elde edilen anatomik bilgilerin füzyon yöntemleriyle operasyon sırasında anjiyo görüntüleriyle birlikte gösterilebilmesi için sağlıklı bir çakıştırma işlemine gereksinim vardır. Çakıştırma parametreleri MR hacminin en büyük yoğunluk iz düşümleri ile 2 boyutlu anjiyo görüntüleri arasındaki karşılıklı yoğunluk bilgisine dayanan bir en büyütme yöntemiyle hesaplanmıştır. İki modalite arasında karşılıklı bilgi miktarını ölçmek için floroskopik görüntü ile MRdan gelen projeksiyon görüntüsünü karşılaştırıldı. En iyi sonucu yakalayan iteratif bir otomatik çakıştırma algoritması oluşturuldu. Algoritma daha once hayvanlardan alınan in vivo floroskopi ve MR görüntülerini kullanarak test edilmiş, yöntemimizin yüksek doğrulukta bir çakışmakta sağlamakta olduğu gösterilmektedir.

Anahtar Sözcükler: Görüntü Destekli Tıbbi Müdahaleler, X-ışını ve MR Görüntü Kaynaştırılması, Yoğunluk Tabanlı İmge Çakıştırma, Hibrid (MRG-XF) Görüntüleme Sistemleri

TABLE OF CONTENTS

LIST OF FIGURE

LIST OF TABLES

LIST OF SYMBOLS

A	image matrix A
B	image matrix B
p_A(a)	Probability distribution of A
p_B(b)	Probability distribution of B
p_{ab}	Joint probability distribution between sets a and b
I(A,B)	Mutual information between A and B
H(A)	Histogram of image matrix A
H(B)	Histogram of image matrix B
$\widehat{u}$	array of the x values on image matrix
Δ s	Quantization value

LIST OF ABBREVIATIONS

MIP	Maximum Intensity Projection
PET	Positron Emission Tomography
CT	Computed Tomography
MRI	Magnetic Resonance Imaging
XFM	X-ray Fused with MRI
XMR	Hybrid Magnetic Resonance(MR)/ X-ray suite
DRR	Digitally Reconstructed Radiograph
XF	X-ray Fluoroscopy
DRR	Digitally Reconstructed Radiograph
DRR	Digitally Reconstructed Radiograph
PA	Primary Angle
SA	Secondary Angle
SID	Source to Image Distance
IS	Intensity Size
FOV	Field of View

1. BACKGROUND

1.1 Image Guided Interventions

With the development of the biomedical technologies in the medical world, physicians are able to diagnose and treat patients increasingly with minimally invasive techniques. Standard X-ray Fluoroscopic Imaging (XF), Computed tomography (CT), or Magnetic Resonance Imaging (MRI) help us diagnose even the smallest abnormalities inside the body and allows us to treat them using special catheter devices.

1.1.1 X-ray Guided Interventions

X-ray is the most common tool used in diagnostic medicine which were first observed and documented by Wilhelm Conrad Roentgen in 1895. Roentgen found it by accident when experimenting with vacuum tubes. This rays were called "X" by the Roentgen to indicate it was an unknown type of radiation.

X-ray imaging (XF: X-ray fluoroscopy) technique is based on continuous imaging using X-rays passing through the body and using a film or a detector. If the body part is dense enough ray does not pass through it (i.e. bone structures), and if it's not dense, rays pass through it. Contrast of the image is depending on the density of the structure. For instance, bones are the most opaque structures, therefore, we can see bones as the most brightest structure on the image. Tumors are also relatively dense than other tissues in the body. Moreover, with the help of radio-opaque X-ray contrast agents we can investigate many other parts of the body like vessels, stomach, colon etc. We can see the flow of the radio-opaque material through vessels/chambers and capture it in real time with XF.

X-ray's are used commonly in medical practice. Images can be used to study

broken bones, inspect dental cavities, detect foreign objects in the body (i.e bullet). In addition we can see moving organs like gastrointestinal track or heart due to its high frame rate.

For cardiovascular interventional studies XF is the gold standard because of its high temporal and spatial resolutions. It also provides relatively modest cost solution, and user friendly environment for operations. XF guided interventions used routinely in many different applications in brain or heart.

1.1.2 CT Guided Interventions

In recent years CT became the gold standard in the diagnosis of a large number of different diseases such as cerebrovascular accidents, intracranial hemorrhage and pulmonary embolism. We can acquire cross-sectional images of the body which could be combined to give the full 3D volume. Relatively high spatial resolution and scan speed of CT allow excellent imaging of the proximal coronary arteries. Technologic improvements makes CT guided interventions easy to use [40]. CT fluoroscopy (CTF), although slower than single frame XF, could be operated "real-time" acquisition mode which physicians employ for interventional operations. However radiation exposure, and lack of soft tissue contrast are the main drawbacks of this technology [24].

CT fluoroscopy allows real-time acquisition and display cross-sectional images. In biopsy procedures CT-fluoroscopy makes it possible to visualize the needle trajectory from skin entry to the target point, performing the procedure more effectively and rapidly [13]. Real-time CT fluoroscopy is valuable in assisting thoracic drainage procedure and guiding transbronchial needle aspiration [47]. It is a very well known technique for abdominal procedures, especially in biopsy [37]. Although CT fluoroscopy is a useful targeting technique, there are some concerns about the technique such as; significant radiation exposure to the patient and the scattered exposure to staff. It is shown that CT fluoroscopy expose higher radiation than other methods and some preventing methods are proposed to decreased scattered exposure [24, 31, 37].

Figure 1.1 Combination of a 16 slice CT, and X-ray Fluoroscopy. Advantage of CT on acqusition of cross-sectional images of the body which could be combined to give the 3D volume, and practical use of XF combined together. [10]

1.1.3 MRI Guided Intervention

Magnetic Resonance Imaging (MRI) is used in diagnostic purposes for many years in medicine. MRI provides excellent soft tissue contrast and does not have any known hazardous effects. In addition to anatomic imaging MRI provide functional information of the body [7]. Therefore, MRI is very useful in oncological, neurological, and cardiovascular diseases. Recent studies shows us that we can use MRI for image guided medical interventional operations. [1, 2, 3, 29]

New generation MR scanners made significant improvements for interventional purposes. They have shorter bores to make operation easier and real-time pulse sequences for faster imaging. Under MR-guidance Speuntrup et al. [39] placed the stent to coronary artery which is a challenging intervention because of the artifacts due to respiratory and cardiac motions. They use an ultrafast, real-time MR imaging technique that combines steady-state free precession for high signal to noise ratio, and radial k-space sampling for motion artifacts. They succeeded this procedure in ten of eleven trials.

Godart et al. succeed MR-guided balloon angioplasty of stenosed aorta. They have used a fast low angle shot (FLASH) sequence, and MR compatible catheters [14]. They use a 0.2 T open MR scanner,T1-weighted fast low-angle shot (FLASH) sequence: TR/TE 120/14 msec, flip angle 30–50°, one slice, field of view (FOV) 190 380 mm, 10 mm slice thickness, matrix 105 256, one acquisition, and bandwidth of 39 Hz/pixel. The resultant acquisition time was 10–15 seconds. Experiment done on 5 piglets and they successfully applied the balloon angioplasty procedure on all of them.

McVeigh et al.[28] used MRI to guide a placement of a prosthetic aortic valve in the beating heart via direct apical access in eight porcine hearts. A clinical bioprosthetic valve affixed to a platinum stent was compressed onto a balloon-tipped catheter. This was fed through a 15-18 mm delivery port inserted into the left ventricular apex via a minimally invasive incision. They use a real time steady state free precession (SSFP) sequence with following scanning parameters: TR = 3.5 ms, TE = 1.75 ms,

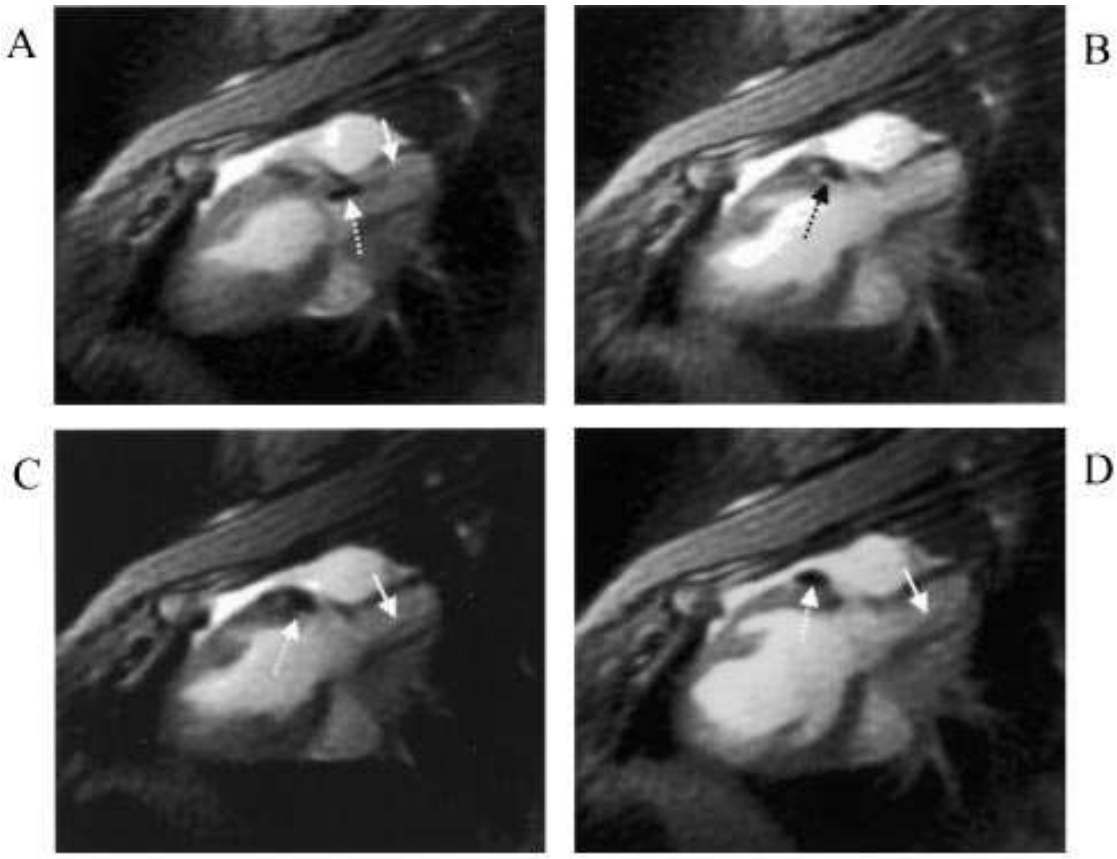

Figure 1.2 Real-time rSSFP images of MR-guided left coronary artery stent placement (A–D). The 0.018-inch guidewire (solid arrow) causes a slightly smaller artifact compared with a 0.035-inch nitinol guidewire. The mounted stent gives a larger artifact (dashed arrow) than the guidewire. [39]

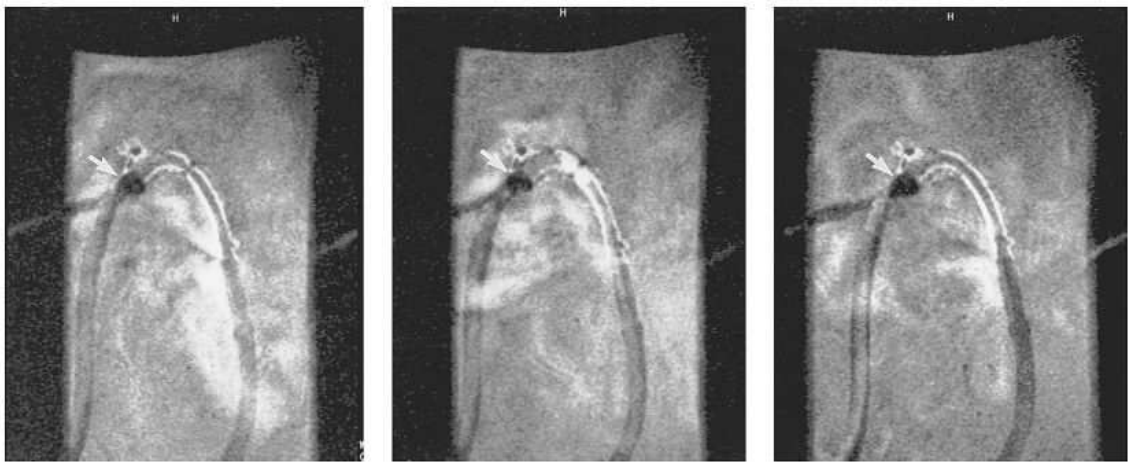

Figure 1.3 In vitro model. Sagittal view (white arrows in all three panels: artifact of the marker on the tip of the nitinol guidewire). Left: Creation of a dilatable stenosis on a porcine segment of aortic arch connected to the plastic tubes. Middle: Angioplasty by a fully pressurized balloon. Right: Complete resolution of the stenosis after dilatation. [14]

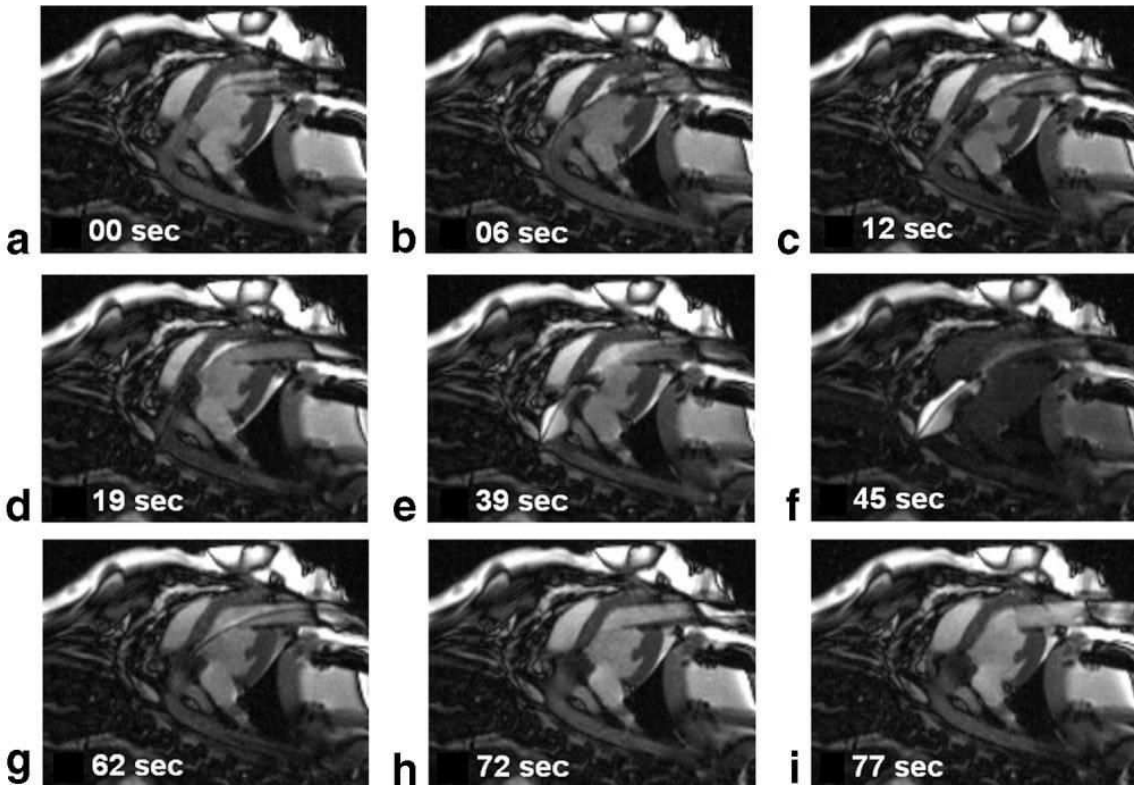

Figure 1.4 Selected frames from the real-time MRI displayed within the scan room, showing the deployment of the prosthetic valve. **a)** A guidewire is advanced through the trocar across the native aortic valve. **b)** The prosthetic valve is advanced to the end of the trocar. **c)** The prosthetic valve is advanced into position in the LV outflow track. **d)** The prosthetic valve is inserted across the native valve and aligned with the coronary ostia and the aortic annulus. **e)** A balloon filled with dilute Gd-DTPA MR contrast agent is used to expand the prosthetic valve. **f)** Interactive saturation is used to enhance visualization of the extent of balloon inflation. **g)** The balloon is taken down and pulled back through the trocar. **h)** The guidewire is removed. **i)** The delivery device is removed from the trocar. The total time required for this sequence of pictures was 77 s. [28]

flip angle = 35-45^{0}, slice thickness = 7 mm, field of view = 340 mm x 255 mm, and the matrix size is 192 x 108. Surgeon implanted the prosthetic valve in the correct location at the aortic annulus less than 2 minutes.

Kuehne et al.[23] placed nitinol stents in the pulmonary valve and main pulmonary artery in five pigs by using MR imaging guidance. For interactive MR imaging monitoring of catheter manipulation and stent delivery, they have used balanced fast field-echo and T1-weighted turbo field-echo sequences. For visualization purposes of the delivery system was based on T2* (with air as the contrast material) or T1 (with gadodiamide as the contrast material). After stent deployment, the position and morphology of and flow through the stent were verified with multiphase multisection balanced fast field-echo and velocity-encoded cine MR imaging.

In other various studies interventional operations, such as transluminal or stent deployment have been successfully conducted under MR guidance [5, 30].

On the other hand MRI guided medical interventions has many disadvantages; The most important one is the lack of MR compatible devices. When a catheter device enters the body during MR imaging, significant temperature increase could be observed on metal containing catheters. In addition because of the shape of the bore, interventional operations suffer from difficulties due to patient access and monitoring. Another disadvantage is its relatively low spatial and temporal resolution in comparison to XF, CT.

In this study we use image registration techniques to fuse a priori MR images on live XF images to get the best of both modalities. A brief overview of registration methods is given next with applications in XFM.

1.2 Overview of Image Registration

Image registration is the process of overlapping two or more images of the same scene taken at different times, from different viewpoints, and/or by different sensors. It geometrically aligns two images: the reference and target images. Image registration is a crucial step in all image analysis tasks in which the final information is gained from the combination of various data sources and used extensively in image fusion and multichannel image restoration. Registration is required in remote sensing (multispectral classification, environmental monitoring, change detection, image mosaicing, weather forecasting, creating super-resolution images, integrating information into geographic information systems), , in cartography (map updating), and in computer vision (target localization, automatic quality control), to name a few [49].

In medical imaging all devices has advantages and disadvantages. For example MR provides high resolution in soft tissues, but it acquires images relatively slowly. On the other hand, X-ray imaging gives us very high spatial and temporal resolutions

but it suffers from lack of soft tissue contrast. Characteristics of these two types of medical imaging modalities make them highly complementary. We could eliminate these disadvantages if we to combine the results coming from both modalities.

Computer tomography and MRI data could be combined to obtain more complete information about the patient; Few more examples are monitoring tumor growth, treatment verification, comparison of the patient's data with anatomical atlases. Registration of different modalities gives us a more complete information about patient. If we use only one modality there are always disadvantages but by fusing two or more modalities we are able to take all the necessary information in a more detailed way. accurate and in a short time. Several registration tools have been used or could be used for image fusion. These will be introduced briefly in the following subsections.

Fusion of information from different modalities using registration algorithms could help physicians during interventional operations by providing them both anatomical, and functional information.

1.2.1 Point-Based Registration

The most reliable registration method uses points which are obtained using internal or external markers [20, 27, 41]. Point-based registration computes rigid transformation matrix which aligns two point sets to each other. It is accurate, fast and robust, thus it is routinely used as a gold standard to evaluate other registration techniques. One major disadvantage of point-base registration is that it is vulnerable to movement of markers when attached to the body. Current XFM registration technique uses point-based registration, and automatically register two modalities [38]. This algorithm is more detailed in section 1.5.1.2.

1.2.2 Feature Based Registration

Feature based methods find correspondence between image features such as points, lines, and contours [19]. Although feature based registration consists of many different approaches; they consist of four basic steps:

- Feature detection, where salient and distinctive features are detected.
- Feature matching, where the feature correspondences between the images are established.
- Transform model estimation, in which the transformation parameters are determined from the the correspondences between the images.
- Image transformation, where the images are aligned.

The main goal on feature based registration is to establish correspondence between two sets of features. The main problems on this technique are: incorrect feature detection and image distortion.

One registration is achieved images coming from different modalities could be viewed on the same coordinate system and visualized using image fusion techniques.

1.3 Intensity Based Registration

Intensity-based registration algorithms match the intensities of two images, find a similarity metric, and register two images. It is generally used for similar modalities such as X-ray fluoroscopy and CT. For 2D 2D registration intensity based registration algorithm iteratively optimises 3 parameters describing the orientation of 2D datasets. 2 parameters are for x and y translation and the other one is for rotation. Figure 1.6 is an example for 2D 2D intensity based registration from XFM project.

Figure 1.5 Feature-based human retina image registration. Registration uses vessels on retina as features. Refer to section 1.2.2 [6]

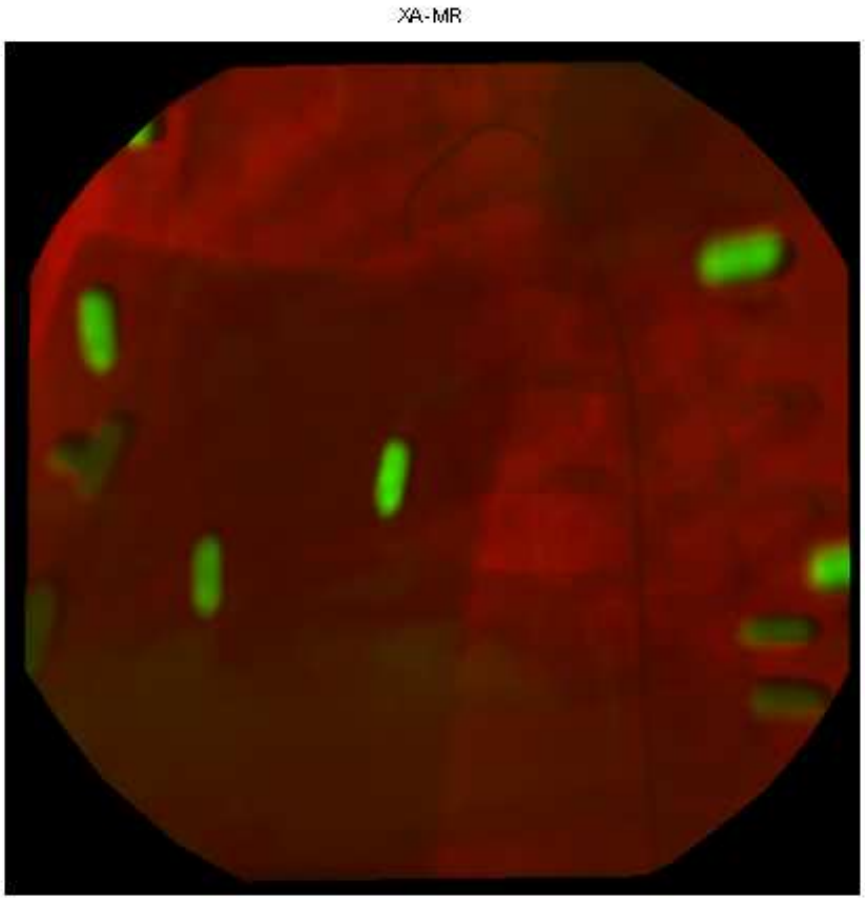

Figure 1.6 2D 2D registration algorithm example from a previous work on my XFM project. Green field is visualize MR, red field is for XF. Translation parameters on x and y axes are shifted iteratively with step sizes dx and dy, according to mutual information.

For 3D to 2D registration algorithm iteratively optimizes the six rigid-body parameters describing the orientation of the 3D datasets. 3 of the parameters are used for translation on x,y,z axes, and the other 3 is for rotation parameters [32].

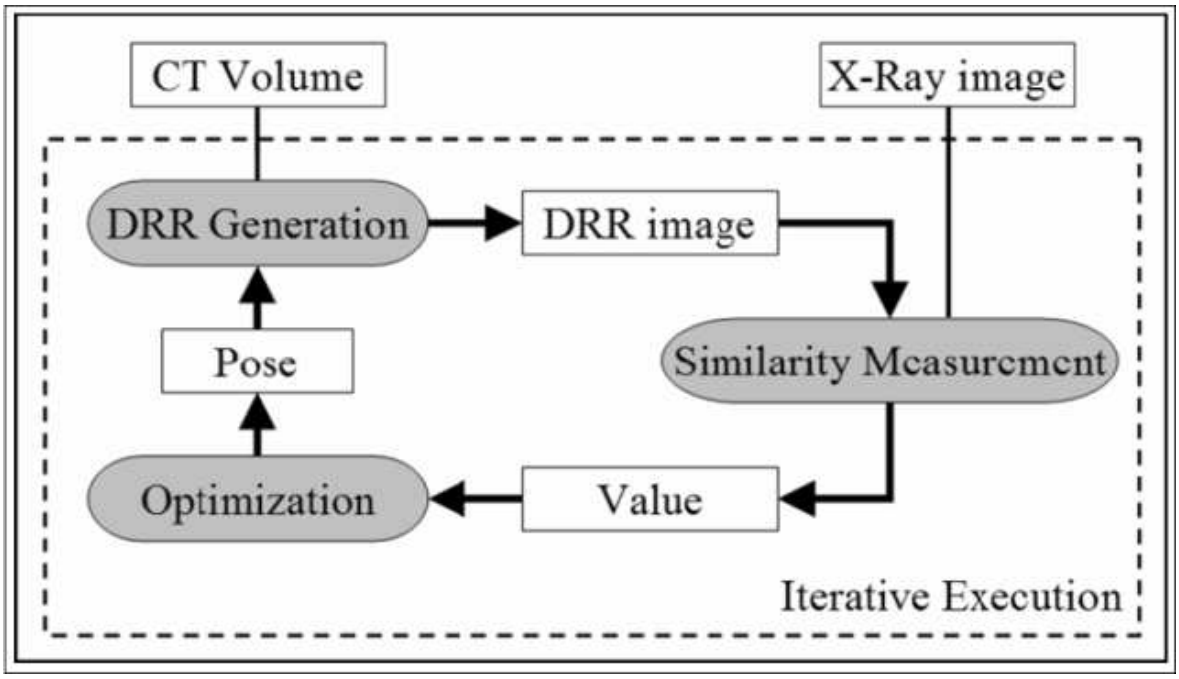

Figure 1.7 Iterative algorithm for 2D-3D intensity-based registration of X-ray and CT images. Refer to section 1.3 [45]

The algorithm for a basic intensity based registration is as follows, in Figure 1.7 intensity based flow chart is explained:

- User gives the system images of two modalities.
- Using a projection technique, one of the image computed from the other. For instance, Digitally Reconstructed Radiography (DRR) image is computed from CT image.
- Alignment of images are identified by a similarity measurement technique.
- Output of similarity calculation used as a cost function of an optimization algorithm, which we try to find out the optimum transformation where two modalities has the maximum similarity between each other.

The basic drawback of the intensity-based registration is that the need of many comparisons, many different projections of DRR's which means we need more computation time [32].

1.4 Image Fusion Techniques in Medical Applications

1.4.1 PET-CT Fusion

PET/CT is the combination of PET (positron emission tomography), and CT (computed tomography) in a single machine. The individual scans, which are taken consequently, could be presented seperately or as a single overlapping, or fused image. The two techniques present different type of information about the human body: PET shows functional information (metabolic or chemical activity in the body); CT shows anatomical structure of the body. So by combining them we can understand the exact anatomical location of a "functioning structure" of the body. PET-CT fusion imaging with the radiotracer Flourodeoxyglucose (FDG) enables the collection of both biological and anatomical information during a single exam, with PET picking up metabolic signals of tissues and CT guide to a detailed map of internal anatomy [22, 44] Figure 1.8 shows us an example for bot PET and CT modalities and a registered PET-CT image. .

Since the images are taken so close to each other while the patient is at stand still and since the system is calibrated registering is not a challenge in this setup.

1.4.2 CT/MRI - Ultrasound Fusion

Registration of ultrasound images to three-dimensional tomographic modalities is receiving a lot of attention especially in neurology and orthopedics. Ultrasound uses information comes from CT/MRI as a pre-operative guide. It is useful for head and neck cancer identification of metastatic neck lymph nodes [48]. Previously computed

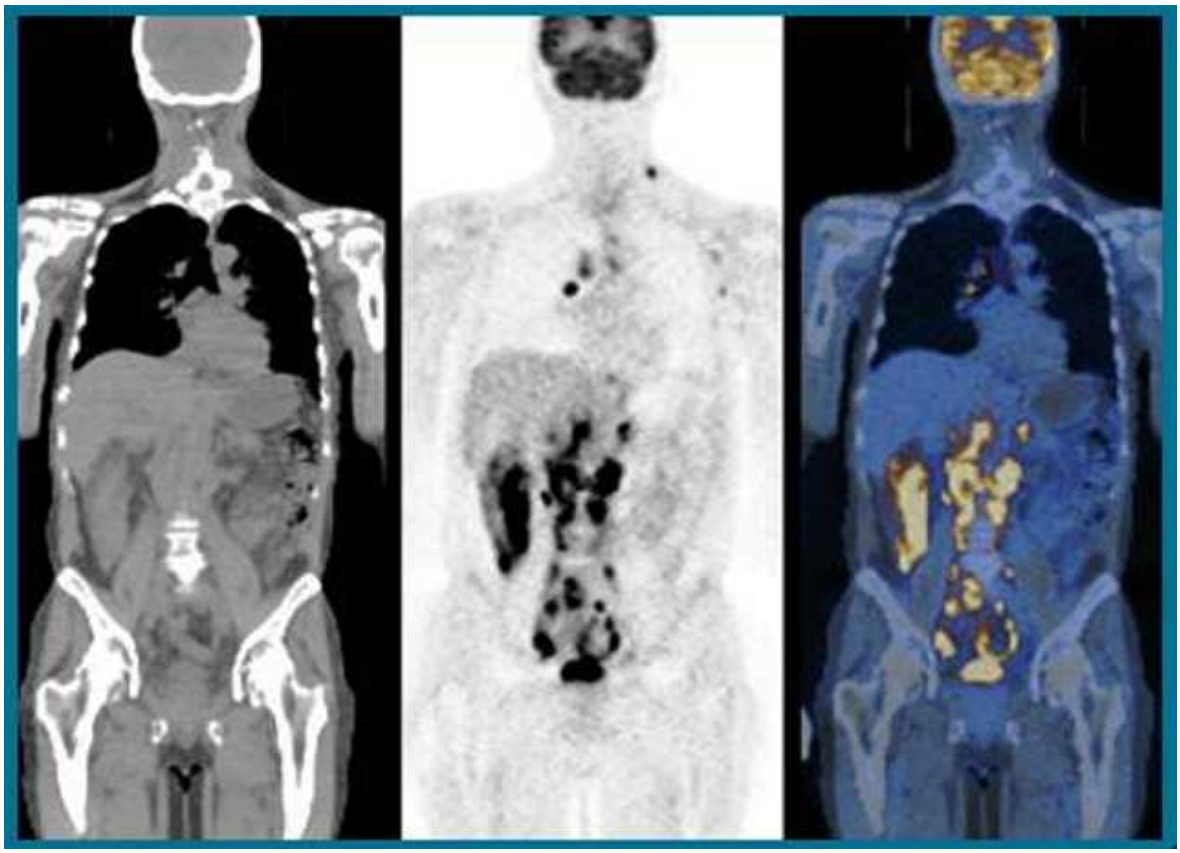

Figure 1.8 Registered PET-CT image. PET-CT has a wide usage area for cancer diagnostic. Since two hardware are attached to each other registration process is relatively easier and faster. Image (A) is CT image, image (B) is PET image, image (C) is CT fused PET Details are in section 1.4.1

4-D CT data stored with original voxel intensity, and for each pixel, the 4-vector is computed from the volume using trilinear interpolation. After a canny-edge detection algorithm is applied to the image, computer makes a similarity measurement and finally registration is done [46].

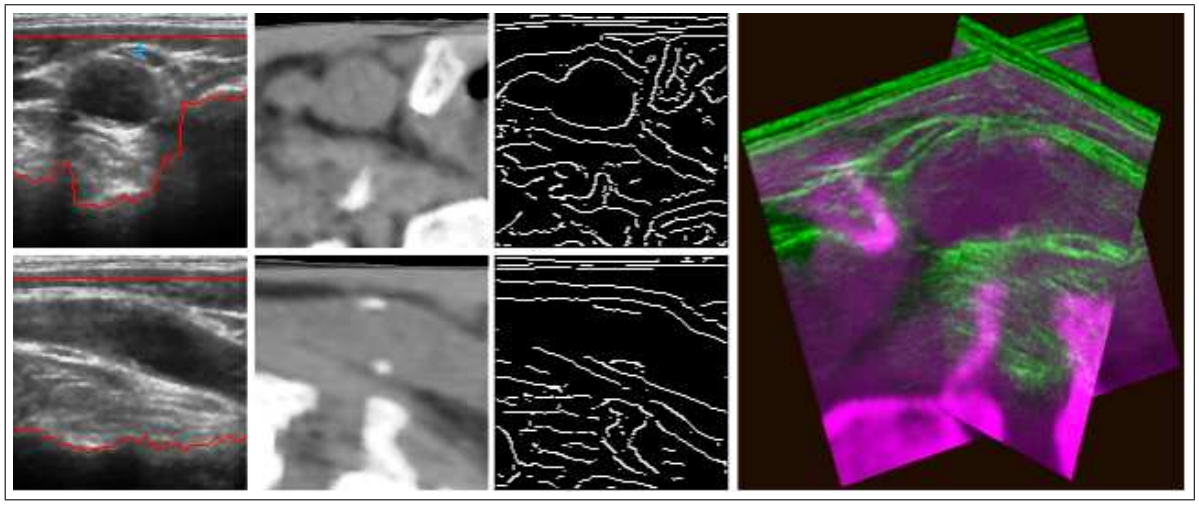

Figure 1.9 Two ultrasound images with ROI (red lines) and target, corresponding CT slices, edges from CT, and overlay in 3D. The physical image size is 4 by 4cm [46].

2. X-ray Fused with MRI (XFM)

Physicians use X-ray fluoroscopy (XF) to visualize the body especially in arteries and veins using contrast agents. During interventional studies XF provides us high spatial and temporal resolution images and a fast refresh rate, which is very useful for catheter based operations. However, as a trade off, XF does not have sufficient soft tissue contrast. X-ray attenuations of the body structures, other than bone, are very close to each other. Therefore, it is so hard to diagnose the body structures under the XF. Additional disadvantages of the XF are potential use of high dose of ionizing radiation and employment of radio-opaque contrast agents to which some patients react unfavorably. On the other hand MR imaging provides detailed anatomical images, excellent soft tissue contrast and could acquire full 3D images or 2D images at arbitrary orientations. MRI has also several disadvantages: it is a much slower acquisition method than XF, it has relatively lower spatial resolution and it is very sensitive to motion during image acquisition. Furthermore, most of the catheters and other tools used during the surgery or intervention are not compatible with the high magnetic field of an MR scanner.

Since the two imaging modalities are complementary to each other, our approach is registration of the images acquired from the two modalities and displaying the fused images during XF-guided interventional studies. X-ray fused with MRI (XFM) combines the strengths of both modalities to improve quality of image guidance. In this system, a prior MR images of the subject are overlaid on top of the live images acquired during X-ray fluoroscopy.

X-ray images provides us very high temporal and spatial resolution in a short period of time. On the other hand, MRI has soft tissue contrast and 3D high-detailed anatomical information. These strong points makes X-ray and MRI complementary to each other. Fusion of these two modalities has been proposed to provide greater guidance in catheter-based interventions [25].

In the literature there are two different hardware approaches for XFM. First one is to incorporate a fixed position flat panel XF into a open 0.5T MR scanner [11, 12], other approach is the use of sliding table between two modalities [33, 34].

First hardware approach with open MR and X-ray is making the registration problem relatively easy but limits the applications to the low magnetic field of open-MR systems. On the other hand using a sliding table such as Miyabi sliding table (Siemens, Erlangen, Germany) has an easier process on hardware but as a trade of software problems are harder to solve. Miyabi table as seen on Figure 2.1 is a common patient table suitable both for MR and fluoroscopy . It is used for combine transport of patients between angiographic procedures and MR-based interventions. After patient get on the table first MR procedure occurs, and patient slides directly to XF without moving from the Miyabi table. Since the patient does not moving from the table it is easier for both patients, and physicians. Software problem is depends on the sliding of the patient. MR and XF are on different places, which means different points on space. Images coming from two datasets can not register onto each other directly. We need to use registration techniques to find common points on two modalities, and match them onto each other, which is not an easy problem to solve.

2.1 Previous XFM Registration Methods

Although XMR suites, which combine MRI with X-ray fluoroscopy have an important potentional on image-guided interventions, there are not many suites world-wide yet. Challenges on registering MR and XF images is making XMR suites difficult to use on clinical area. Additional difficulties are: distortion correction because of the effect of magnetic field on XF, and limitations of the registration process (it must be fast so that it doesn't add too much overhead to the complex procedures in the XF suite). Registering a 3D MR volume to a 2D X-ray projection is also another main difficulty.

The literature has many examples of registering pre-operative X-ray computed

Figure 2.1 MRI X-ray Imaging (XMR) Suite. They are using a miyabi table for patient transfer between two scanners which helps to transfer patient easily and without movement. All products are MR compatible after images acquired MRI and registered doctor operates on XF [34].

tomography (CT) images with XF [9, 32, 50]. These methods rely on the similar image formation process between the two modalities to create so-called digitally reconstructed radiographs (DRR), which are projections through the CT volume that resemble XF images, to drive intensity-based registration algorithms. MR images have different contrast than CT images, and do not necessarily resemble X-ray images, so these approaches are not easily tailored for XFM.

There are several studies on 3D-to-2D MR–X-ray registration [42, 8, 35], which have shows us theoretical methods, but clinically these are not sufficient. Fahrig et al. were able to integrate a stationary flat-panel XF system within an open 0.5 T MR scanner, so the registration of both systems is constant and does not need to be repeated across experiments [11, 12]. However, the single, fixed-angle XF view is a huge limitation for many vascular interventions, and the low field magnet has a lower signal-to- noise ratio compared to the more commonly used 1.5 T MR systems. Rhode et al. [33] used a mobile cardiac XF system and a 1.5 T MR system joined by a sliding table. However, it has the limitation of registering the imaging systems independently of the patient, so that any patient motion is unrecoverable.

2.1.1 Marker Based XFM Registration technique

When Gutiérrez et al. applied the first registration algorithm, he used a point based registration technique [17]. Algorithm capture the raw X-ray images taken by the XF by using a frame grabber. Because of the raw signal coming from the XF device, there are distortions more pronounced on the edge of the XF images. To solve this problem polynomial based correction function is used to dewarp the images coming to the computer. (For this purpose a capture program which comes with the capture card provided by AccuStream Inc. is used). After dewarping the fluoroscopy images according to dewarping polynomials they pass through a segmentation algorithm for segment the markers on the image. Segmentation of the markers are the key process for registration. On the other side, MR images are taken from the MRI and markers on the images are identified and labeled. After segmentation, numbered MR mark-

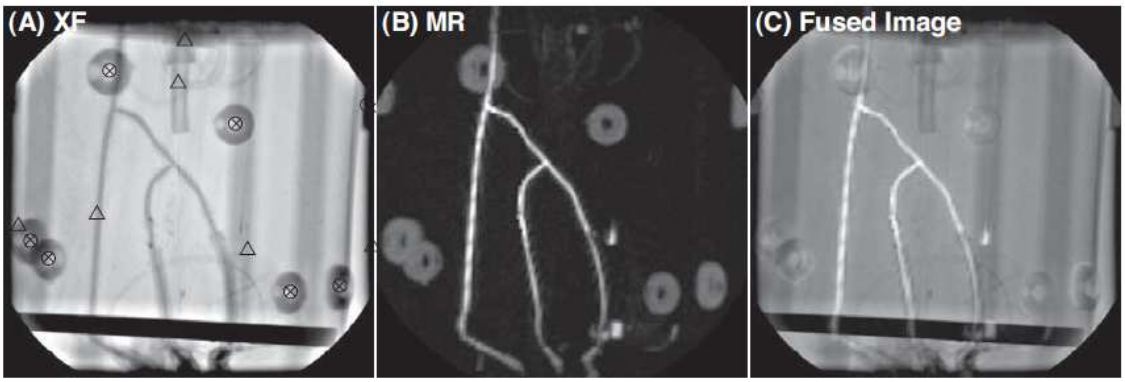

Figure 2.2 3D-to-2D registration: (A) (×) segmented marker positions in the XF image; MR markers (Δ) before and (∘) after registration. (B) Registered perspective MIP of the 3D MRI. (C) Fused image of MRI MIP and the XF image[15]. Marker based registration technique explained in section 1.5.1.1.

ers are matched with the markers on the angio side manually. After matching of the same markers on two different modality an optimization algorithm is run for the registration. Optimization algorithm basically calculates the distance between two point sets (coming from coordinates), fiducial marker, and try to minimize the distance by changing translation and rotation parameters of a rigid body transformation in 3D. After calculation of 6 parameters of this transformation (3 rotation, 3 translation) from points. Algorithm applies the parameters to the MR images or any region or volume information and fusion is accomplished.

2.1.2 Automatic Marker Matching

In 2008, Sonmez et al. develop an algorithm which is a complimentary for Gutierrez's marker based registration technique [38]. Aim of this algorithm is to simplify the registration steps for routine clinical use by making the system fully automatic. This automatic marker matching method calculates the similarity between all possible fiducial markers matches coming from two modalities, and by evaluating all these similarity results software identifies the fiducal marker matches automatically. This algorithm encompasses these modules: detection of markers in both MR and X-ray images, reconstruction of 3D position of markers in rotating X-ray views and finding correspondence between 3D point sets automatically. More details are provided within the rest of this subsection.

In order to go from 2D X-ray images to the physical 3D space, and to overcome the problem of the overlapping on markers on certain X-ray scenes, multiple X-ray images from different views are acquired. After identification of markers in both MR and X-ray images, these points sets could be matched with a unique algorithm especially designed for this purpose [38]. Correspondence between points sets, come from X-ray and MR, is based on triangle similarity. As we know three non-collinear points on a 3D space determine a unique triangle. Marker positions are used for corner points and all possible triangle sets were built from marker sets and each triangle from the first set (e.g. X-ray) is compared with all other triangles of the other set (e.g. MR). From the similarity of the triangles a confidence value is obtained for each match and assigned to the corners of these two triangles. A cumulative confidence matrix from all possible matches is constructed, and by using the best match information a 3D to 3D registration was performed.

Two triangles are assumed to be similar if their sides are equal to each others. Let $\Delta 1$ is triangle with sides $(a_1; b_1; c_1)$, it is similar $\Delta 2$ to other triangle, $\Delta 2$, with sides $(a_2; b_2; c_2)$, there is this relationship between matching sides:

$$\frac{a_1}{a_2} = \frac{b_1}{b_2} = \frac{c_1}{c_2} = 1 \tag{2.1}$$

Then $\Delta 1$ and $\Delta 2$ are similar, we use the notation $\Delta 1 \sim \Delta 2$. Since in application points will not be in exact locations because of noise and different imaging modalities formula modified as follows:

$$S_{1,2} = |1 - \frac{a_1}{a_2}| + |1 - \frac{b_1}{b_2}| + |1 - \frac{c_1}{c_2}| \tag{2.2}$$

This similarity value is calculated for each possible condition and the lowest

points gives us the match for two imaging modalities [38].

2.2 Distortion Correction

Images displayed in this thesis were acquired from an Axiom Artis cardiac single plane XF system and a 1.5 T Siemens Sonata MR scanner. MR images used for registration were acquired by using a 3D gradient echo sequence with typical parameters like: TR 2.37 ms, TE 1.18 ms flip angle 17° and FOV 400 x 300 x 230 mm. Matrix size is 256 x 192 x 61 voxels; bandwidth 1300 Hz/pixel. XF system uses conventional image intensifier with 33 cm FOV, and images were acquired in 512x512 pixels format. Before the fusion, it is necessary to apply distortion correction to both XF and MR image sets. Due to magnetic field effect to X-ray beans on X-ray fluoroscopy device we have to apply distortion correction algorithms.

2.2.1 Distortion Correction on MR Images

MR imaging based on linear magnetic gradients within the bore of the magnet, where magnetic field is homogeneous. However, the gradients are non-linear at the edge of the imaging volume and non constant in the z-direction, which causes spatial distortion on the image. These distortions could be corrected easily with console build readily available software supplied by Siemens [21].

2.2.2 Distortion Correction on X-ray images

X-ray images suffer from pincushion and S-shaped geometric distortion, as shown in Figure 2.4. S-shaped geometric distortion is due to local magnetic field and has both rotational and translation components and depends on position of C-arm. Guttierrez in his Ph.D. thesis explains a global solution for X-ray image distortion. Phantom used to for characterization the distortion was a sheet of plastic with metal

rings placed in a regular grid pattern. The rings were segmented for each image. 5th-order polynomial coefficents were determined that the distorted ring image to ideal grid image. Using these coefficent X-ray images could be corrected for a given angle or for a desired range of X-ray imaging parameters (primary angle, secondary angle, source to image distance, intensifier size) within the calibration range.

2.2.3 Geometric Calibration of an C-Arm

When 3D images are projected to 2D images rotational and translational distortions are observed. To correct for the translational ambiguity of the distortion correction an extra translation correction matrix is added to standard projection matrix. 3D to 2D image projection is obtained by the following equations:

$$\begin{bmatrix} x_n \\ y_n \\ z_n \end{bmatrix} = \begin{bmatrix} -I_i \frac{SID}{FOV} & 0 & -I_i/2 \\ 0 & -I_j \frac{SID}{FOV} & -I_j/2 \\ 0 & 0 & 1 \end{bmatrix} \begin{bmatrix} x_m \\ y_m \\ z_m \end{bmatrix} \tag{2.3}$$

and

$$\begin{bmatrix} u \\ v \end{bmatrix} = \begin{bmatrix} x_n/z_n \\ y_n/z_n \end{bmatrix} \tag{2.4}$$

where x_n ,y_n ,z_n refers to XF 2D coordinates in homogenous form,x_m ,y_m ,z_m refers to marker 3D coordinates, I_i and I_j are number of pixel in x and y direction, and (u, v) are the image coordinates after converted from homogeneous coordinates. Gutierrez at el [16] added an extra step to simulate residual in-plane rotation and translation:

$$\begin{bmatrix} u' \\ v' \end{bmatrix} = R' \begin{bmatrix} u \\ v \end{bmatrix} + t'$$

where R' and t' are represent a 2D rotation and translation, (u', v') is the new coordinate due to distortion correction refinement.

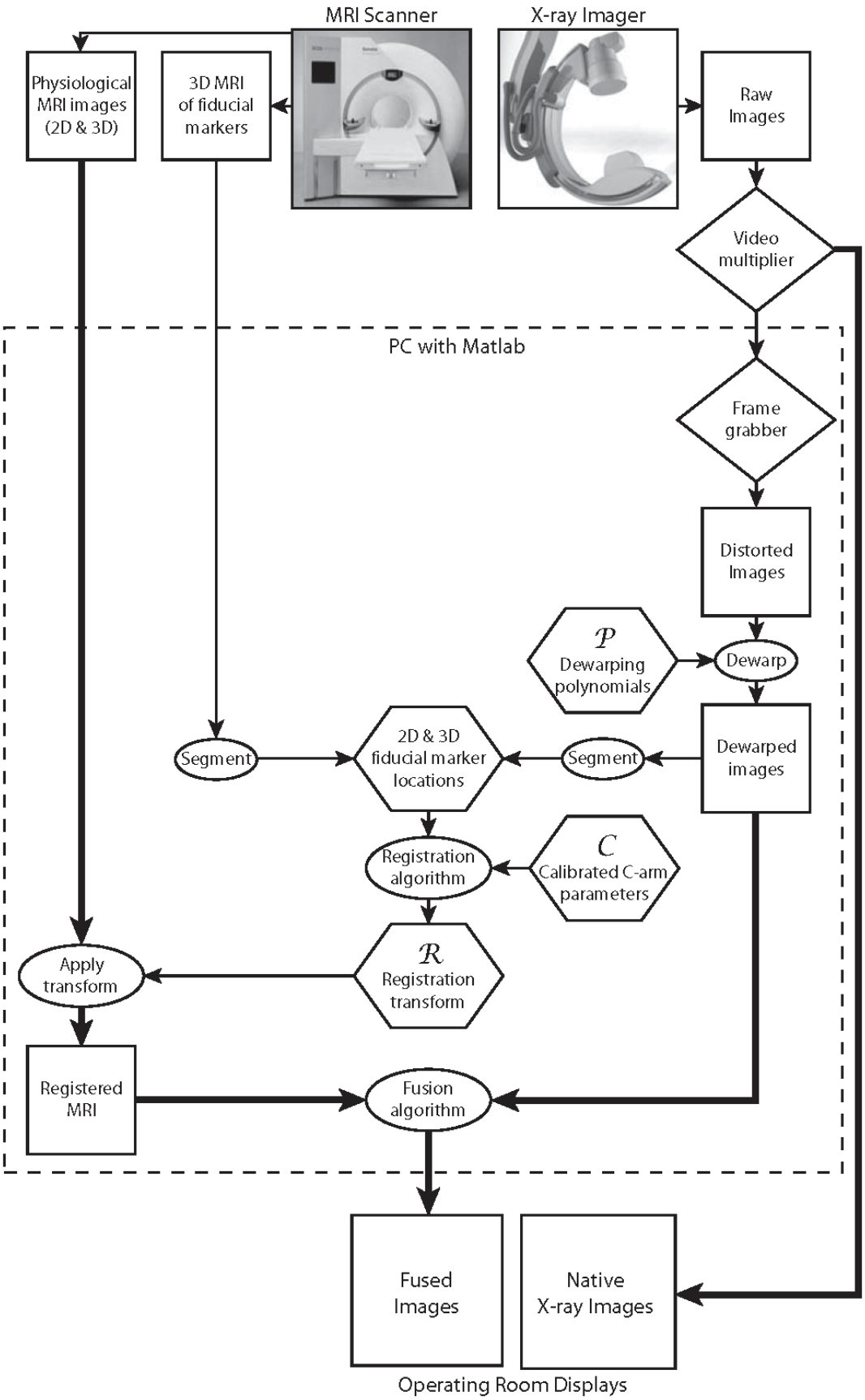

Figure 2.3 Gutierrez flow chart describing the steps involved in registration and fusion of MR and XF images [15].

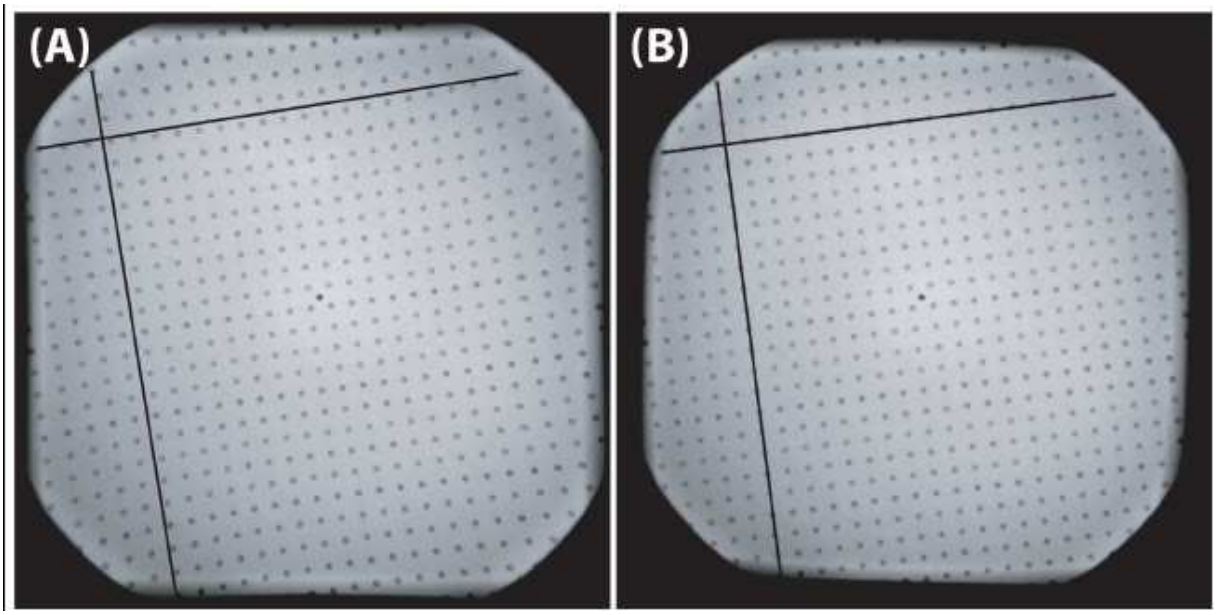

Figure 2.4 Grid phantom is used to observe the distortion characteristic in X-ray images. Image (A) is before and (B) is after distortion correction. Black line is added to highlight the distortion [16].

3. Intensity Based Registration for X-ray Fused with MRI System

3.1 Introduction

In this study our goal is to create a successful intensity based registration algorithm to reduce the dependency on markers. For this aim we try to register a 3D MR volume to a 2D XF image. For this, we create a 2-D fan beam style projections of the MR image according to the specifications of X-ray image. We calculate mutual information similarity between two modalities. The whole approach will be detailed in this section.

3.2 Methods

Our aim is to find the position and orientation of the MR image with respect to an XF image. There are basically 4 different types of relevant parameters in this problem. First ones are the translation parameters (T_X,T_Y,T_Z). Second group is the rotation parameters (R_θ, R_ϕ, R_ψ). Third group parameter is the pixel sizes of the images which is known for both modalities. Since we are using 2 different modalities we need to equalize the size of two images. So the registration is done in "real space" where coordinates are in mm not pixels/voxels. Last group is the parameters that belong to X-ray fluoroscopy machine which gives us the basic measurements about the position of the patient, position of the detector, intensity size, calibration parameters. We take this last part directly from a previously calibrated XF machine.

3.2.1 Maximum Intensity Projection

Maximum intensity projection (MIP) is a computer visualization method which creates a 2D projection image from a 3D volume data using ray tracing techniques as shown in Figure 3.1. The MIP image is created by selecting the maximum value along the path of a ray through a 3D volume and assign it to each pixel of the MIP image [36]. A group of rays is passed through the volume and MIP image stores the maximum values along the rays in a projection on that direction. For XFM special projections of 3-D MR volume are needed for each XF slice. Rays starting from the position of X-ray source are passed through the MR volume and the maximum intensity value is found on X-ray paths for each pixel at a given 3D MRI volume positioning; Figure 3.2 visualize the maximum intensity projection algorithm. Please note that the final positioning parameters are not known at the beginning, we start from an initial guess and iteratively search an optimum solution. By this way we are able to create a 2-D projection of the MR volume which is replicates XF image formation.

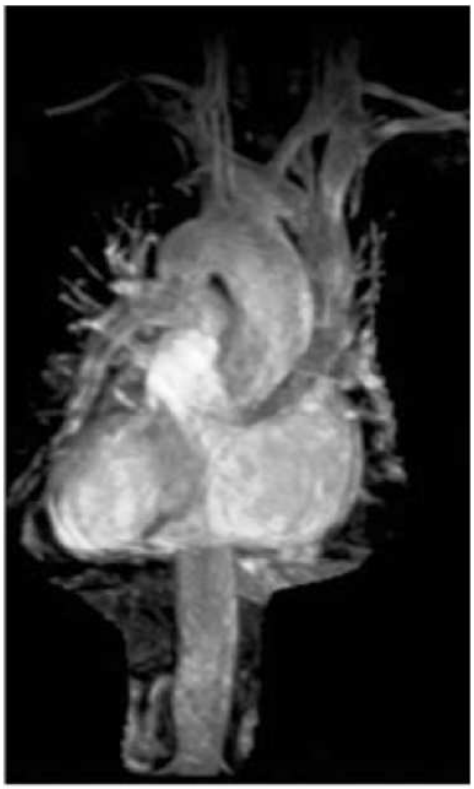

Figure 3.1 Maximum Intensity Projection from contrast-enhanced MR angiography at the level of heart, and aorta [4].

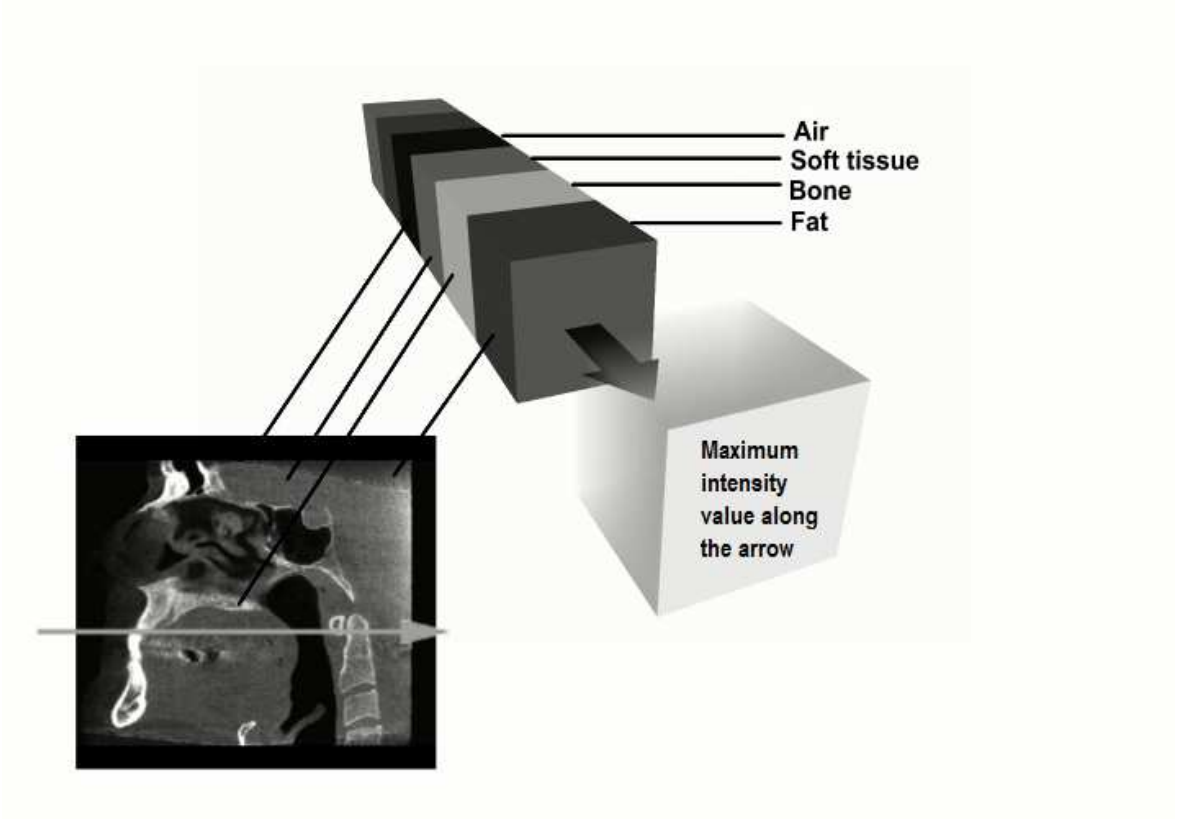

Figure 3.2 Acquisition of a single pixel value during maximum intensity projection (MIP). A single ray passes through several tissues and assumes the highest pixel intensity value. We are using rays passing through the 3D MR volume and we get a 2D projection plane.

3.2.2 Entropy, Joint Histogram & Mutual Information

For intensity-based registration we need to find a similarity metric between two images coming from two different modalities. For this purpose we will use mutual information which will measure the similarity between these two partially dependent data sets. We have two different data sets, which we can define as random variables with marginal probability distributions, $p_A(a)$ and $p_B(b)$, and joint probability distribution, $p_{ab}(a,b)$, are statistically independent if $p_{ab}(a,b) = p_A(a)\ p_B(b)$, while they are maximally dependent if they are related by a one-to-one mapping $T : p_{ab}(a,T(a)) = p_A(a)=p_B(T(a))$. But in our case none of these two arguments are true. We need to calculate the degree of dependence between $p_A(a)$ and $p_B(b)$. For this purpose we will use mutual information which will measure the relation between these two partially dependent data sets. These relation called as "Kullback-Leibler Measure" [43].

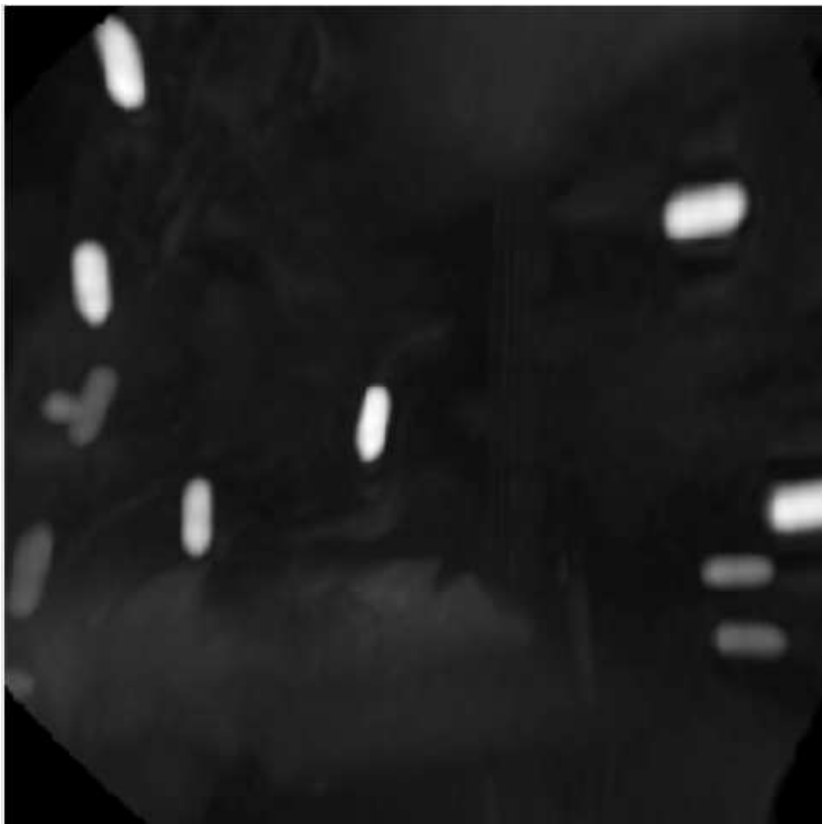

Figure 3.3 Maximum Intensity Projection of 3D MRI volume on XF plane [4].

$$I(A,B) = a,b \sum p_{AB}(a,b) \log \frac{p_{AB}(a,b)}{p_A(a) \cdot p_B(b)} \tag{3.1}$$

"Entropy" is a measure of the unavailable energy in a closed thermodynamic system that is also considered to be a measure of the system's disorder. It is a common term especially used to explain second law of thermodynamic. Entropy can be explained as a measure of uncertainty, variability, and complexity in a general manner. We will use entropy for a measure of variability in our registration algorithm. Joint entropy is a value which shows the similarity between two matrices. It is inversely proportional to similarity of the images. When the similarity between the pixel values increases , the joint entropy starts to decrease. Joint entropy is illustrated with a two dimensional histogram in which x and y projections of 2D pixel density distribution are shown by seperate histograms of two different images as we can see in Figure 3.4.

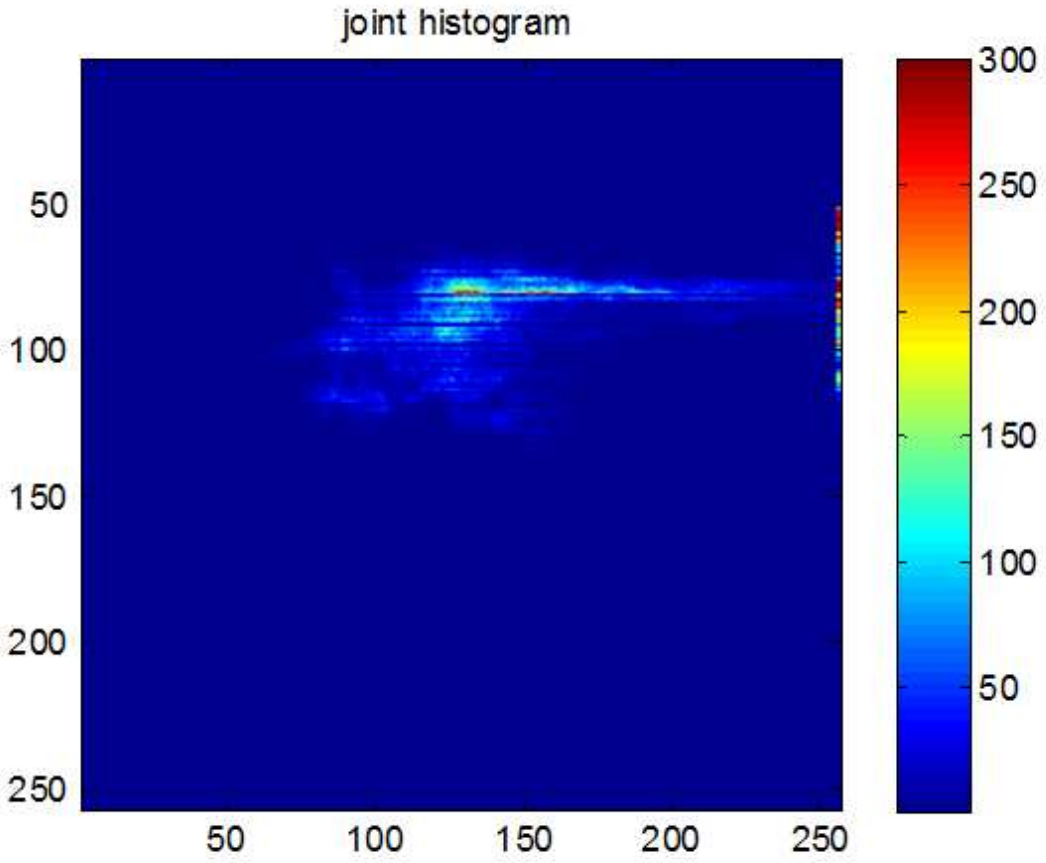

Figure 3.4 Joint Entropy Result of two non registred images

Since joint entropy only shows the value of image parts which come over to each other, we need more general formula. So we use mutual information for calculation which uses joint and seperate histograms of two images. Therefore, we can formulate the entropy and mutual information as below:

$$H(A) = a \sum p_A^T(a) \log p_A^T(a) \tag{3.2}$$

$$H(B) = -b \sum p_B^T(b) \log p_B^T(b) \tag{3.3}$$

$$I(A,B) = H(A) + H(B) - H(A,B) = a,b \sum p_{AB}(a,b) \log \frac{p^T_{AB}(a,b)}{p^T_A(a) \cdot p^T_B(b)} \qquad (3.4)$$

Mutual information is a quantity that measures how much does an image tell us about another. It gives us a similarity value between two images. It is a dimensionless quantity and can be thought of as the reduction in uncertainty about a random variable given knowledge of another. High mutual information indicates a large reduction in uncertainty; low mutual information indicates a small reduction; and zero mutual information between two random variables means the variables are independent. Our main hypothesis is that between similar tissues, even in different modalities, there are similar intensities.

To calculate the Mutual Information, we need two different data set. First one is the X-ray fluoroscopy slice, and the second one is the maximum intensity projection of MR volume taken according to current XF imaging and registration parameters. By using the information that we take from XF slice we are trying to create a 2 dimensional projection of MR image approximately along the assumed X-ray paths. These paths will change when we iteratively change the MR volume during the registration (Figure 3.5).

3.2.3 Intensity Based XFM Registration Algorithm

Our registration algorithm depends on a good starting point. Since there is not very high mutual information between MRI and XF, we cannot start our intensity based registration without a good initial, educational guess. In XFM we start our algorithm by bringing centers of markers together initially to get two modalities close to each other. We use AX image, MR image, and calibration data to correct for distortions in a certain AX image. First we process the MR data; we select the suitable MR data series, and downsampling size of the MR image is routinely selected to speed up the registration. Downsampling ratio is an important parameter for us. We are calculating

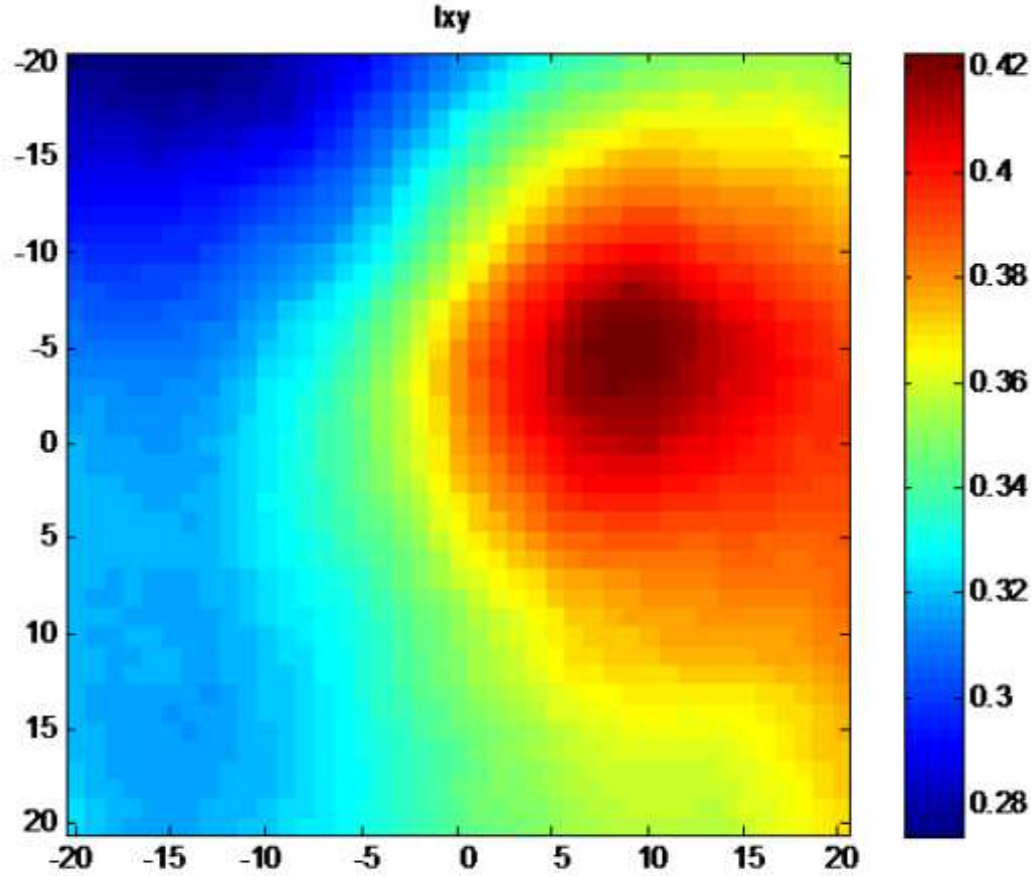

Figure 3.5 Mutual Information between two modalities. When we calculate the mutual information between two modalies we are able to calculate the translation and rotation parameters for to register two images. As we can see the peak point for registration is at (10,-5) pixel from the center of the image. Referred to section 3.2.2.

maximum intensity projections of MR volume according to AX slice as we explain in section 3.2.1, Maximum Intensiy Projection.

After we define our maximum iteration and tolerance function for our optimization code we solve the problem with a non-linear least square optimization method. As seen in Figure 3.6 we calculate new Rotation and translation parameters and create a new registration matrix for iteration. After we calculate the error function according to these new parameters we check out the new registration, and continue to create new registration parameters until our final error function is less than our tolerance value or the change on the error is not changing for several iterations.

3.2.4 Quantization

Quantization is a method for sub-sampling intensity of the digitally reconstructed images, this creates a window of pixel values and assign all pixels in the window into a single value, essentially decreasing the bins of the histogram, decreasing the complexity of mutual information calculation [18]. We use quantization to down-sample our maximum intensity value projection from the MR image. Our two basic reasons are to reduce processing time by reducing the size of the image matrix, and by smoothen the MR images to get better mutual information behavior during iteration. In our studies, we see that 8-bit quantization of MR projection is the best value when comparing with AX images. If the images has a better quality there will be too many local minimum and maximums, which make the registration harder. On the other hand, if the quality is lost due to excessive down-sampling we lose the important intensity information data for our registration algorithm. Quantization is basically approximating a group of pixel values to a relatively small set of discrete values, reducing depth of the image. Different quantization levels and image depths are shown in Figure 3.7.

3.2.5 Preparation of Maximum Intensity Projection

We use the maximum intensity projection to get 2D projections from 3-D MR volume. We use our rigid registration parameters to create a projection of MR. When rotation and translation parameters are correct we should get the highest mutual information value. During maximum intensity projection initial preparation we use rotation and translation parameters from XFM algorithm very similar to previous work by Guittérez [15], which has using ray projections through the MR volume and project maximum intensity values through the ray onto a plane for each position which we are using the initial guess XF coordinate parameters. In this work they only used this for image fusion, we utilize the same concept for registration.

3.2.6 Getting Ready for Registration

After we get fluoroscopy and MR images, the MIP projection of the MRI is calculated according to initial parameters and down sampling ratio. We mask both images to get rid of unused part of the images. Masking has two main reasons; first one is to make less operations during registration, second one is to focus only on the significant part's image intensities rather than any other intensity information present on the images (such as patient name, device information in AX). So we mask the unwanted part of the image. We use a tool for this process it is either used a pre defined mask image, or we can choose our region of interest by hand (Figure 3.8).

3.2.7 Registration

After taking first maximum intensity projection, XF image, and initial registration parameters, we are ready for the iterative optimization. For optimization algorithm we use least square minimization algorithm method "lsqnonlin" of Matlab. This algorithm helps us to calculate optimum registration parameters according to the mutual information error matrix. We calculate the mutual information error by

Registration Properties	
Dimensionality	2D-3D (Time Series)
Nature of Registration Basis (Extrinsic Basis)	Invasive & Fiducial
Nature of Registration Basis (Intrinsic Basis)	Intesity based
Nature Of Transformation	Rigid
Domain Of Transformation	Global
Interaction	Initialization supplied interactive
Optimization Procedure	Parameters computed
Modalities	Multimodality (XF & MR)
Subject	Intrasubject
Object	Thorax (Cardiac)

Table 3.1
Classification scheme for mutual information based image registration technique methods [26].

comparing the XF image and the maximum intensity projection of MR image which is calculated at each step using newly updated registration parameters. If the change in our registration parameters is less than our tolerance value; or maximum iteration number exceeds; it gives out the last calculated registration parameters, for the final registration. We can track our algorithm flow chart from Figure 3.9.

We can define our registration technique as it is classified by Maintz et. al **[26]**. We are making a multimodality registration between MR and CT. Our registration algorithm's dimensionality is 3D to 2D. Nature of registration basis is two fold: we use fiducials for comparison, and from intrinsic intensity-based registration. We are using rigid body transformation. Since we apply our algorithm to the entire image it is in the global domain. Intensity based registration for XFM is a semi-automatic registration technique, which needs initialization for getting images closer to each other on space. Since we do not prefer user interaction to registration program we are using previous course registration algorithm using markers for this purpose.

In optimization procedure parameters computed with least square minimization method. Basically we try to fit a curve to another in multiple dimensions, we calculate the metric "Mutual Information" between two image volumes, than we transform volume, retake the MIP and look for mutual information again. When we end our registration process. Our projection algorithm from 3D X-ray images to 2D and calibration process was explained on section 2.2.3 in detail.

Since all of the images involved in a registration task are acquired from the same patient we can call our registration as an intrasubject registration in our examples given here so, we are dealing with the cardiac anatomy our object is thorax, more accurately cardiac.

3.3 Mutual Information Based Registration Metric

Mutual information error parameter is calculated basically depending on mutual information of the image. Since MI is a dependency value between two images, it changes between -1 to 1. We divide our image into sub-parts to get more detailed results from the image. If a partial similarity on the image exists we recognize it. We shift the values upwards to work in positive scale.

$$I = \{0 : 2\} \tag{3.5}$$

We have chosen to divide our images into several small sub-images, and add a weight constant to our error parameter. A single mutual information from the global image is not adequate since there is no contrast in most of the image regions. By dividing the image into several parts we are able to guide the registration better. Mutual information value is changing between 0 to 2. Assume that we have same random sets, and say that their histogram values are the same. As we can see from

the formulation below maximum value will be 2.

$$H(x) = H(y) = H(x, y) = h$$

$$I = \frac{H(x) + H(y)}{H(x, y)} = \frac{h + h}{h} = 2$$

Initial registration parameters is the weakest point of our algorithm. To obtain mutual information we need at least partially registered objects. Since we don't know the location of the MR-volume on space; if we start from a random point on the space, and cannot get any projection on the plane we cannot able to make iterations. We choose to start from an initial guess using markers available in these datasets. Sensitivity of our registration method to the goodness of this initial starting point is explored further in chapter 4.

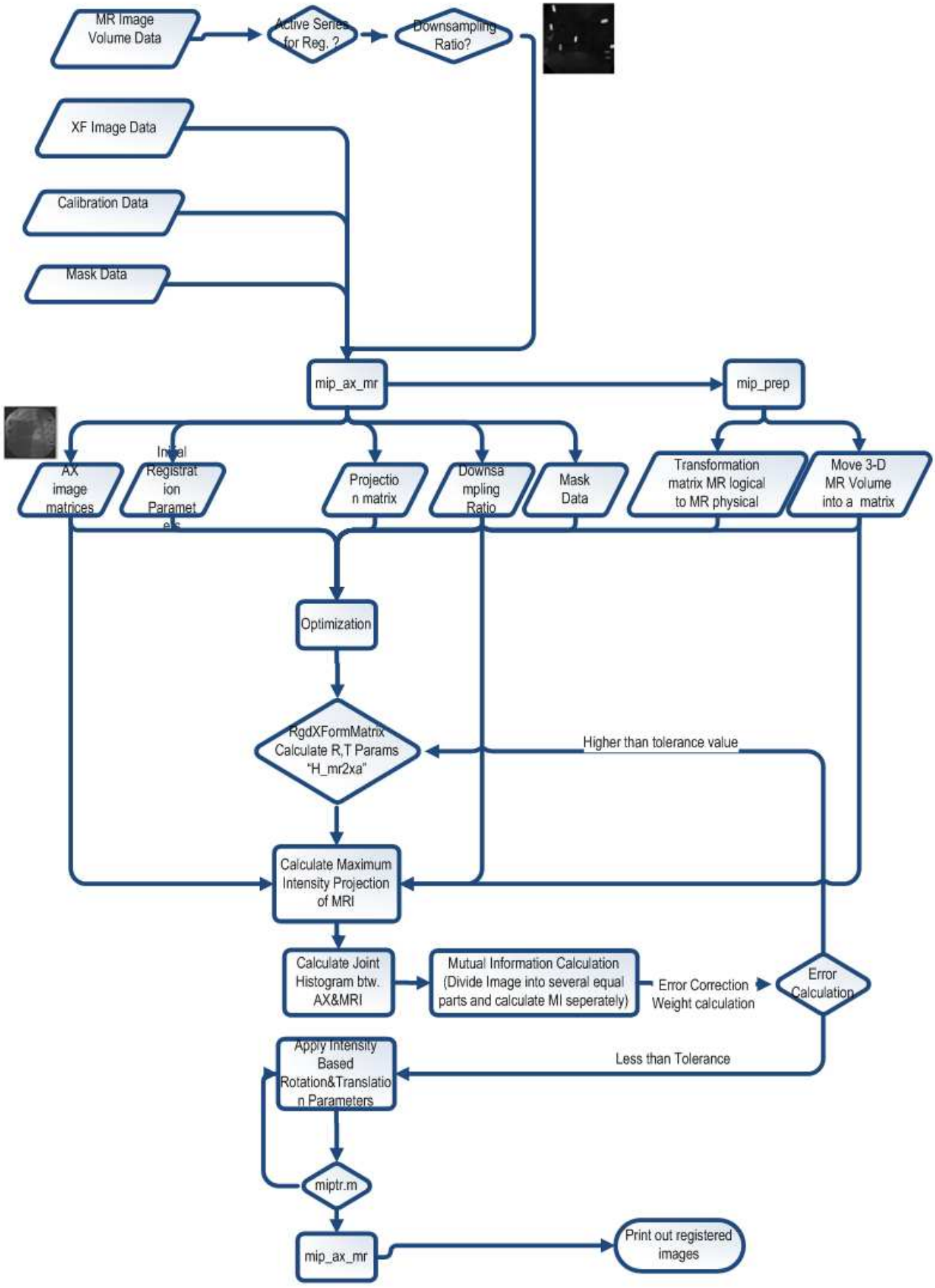

Figure 3.6 Flow Chart describing the steps of Intentsity Based registration Program

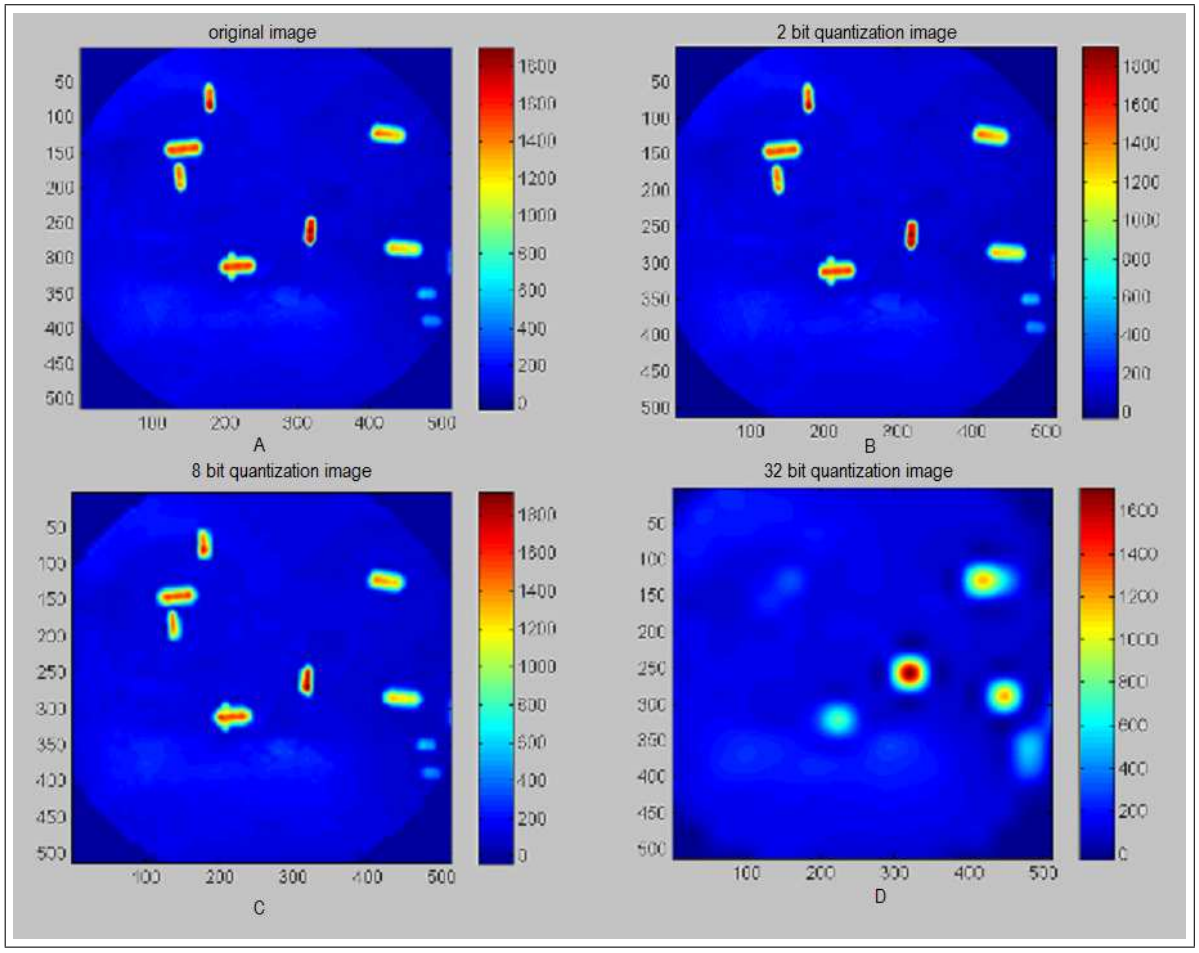

Figure 3.7 Downsampling examples for an MR projection. As the quantization ratio increases detail of the image decreases, that cause lack of intensity values. Our aim is to find optimum quantization value for intensity based registration. a) Original Image b) 2-bit quantized image c) 8-bit quantized image d) 32-bit quantized image

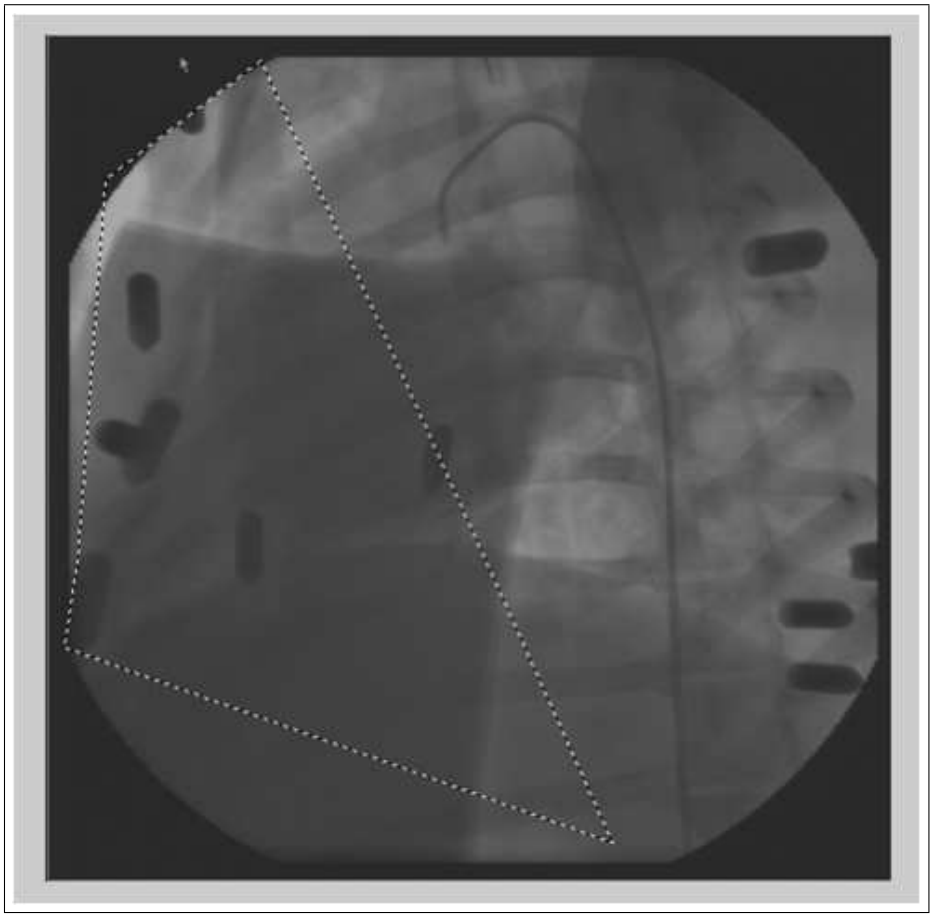

Figure 3.8 Masking Process Of the Image. We generally use presaved mask matrix in our algorithm for time advantage. We cut out the part that doesnot contain useful intensity values for computational purposes.

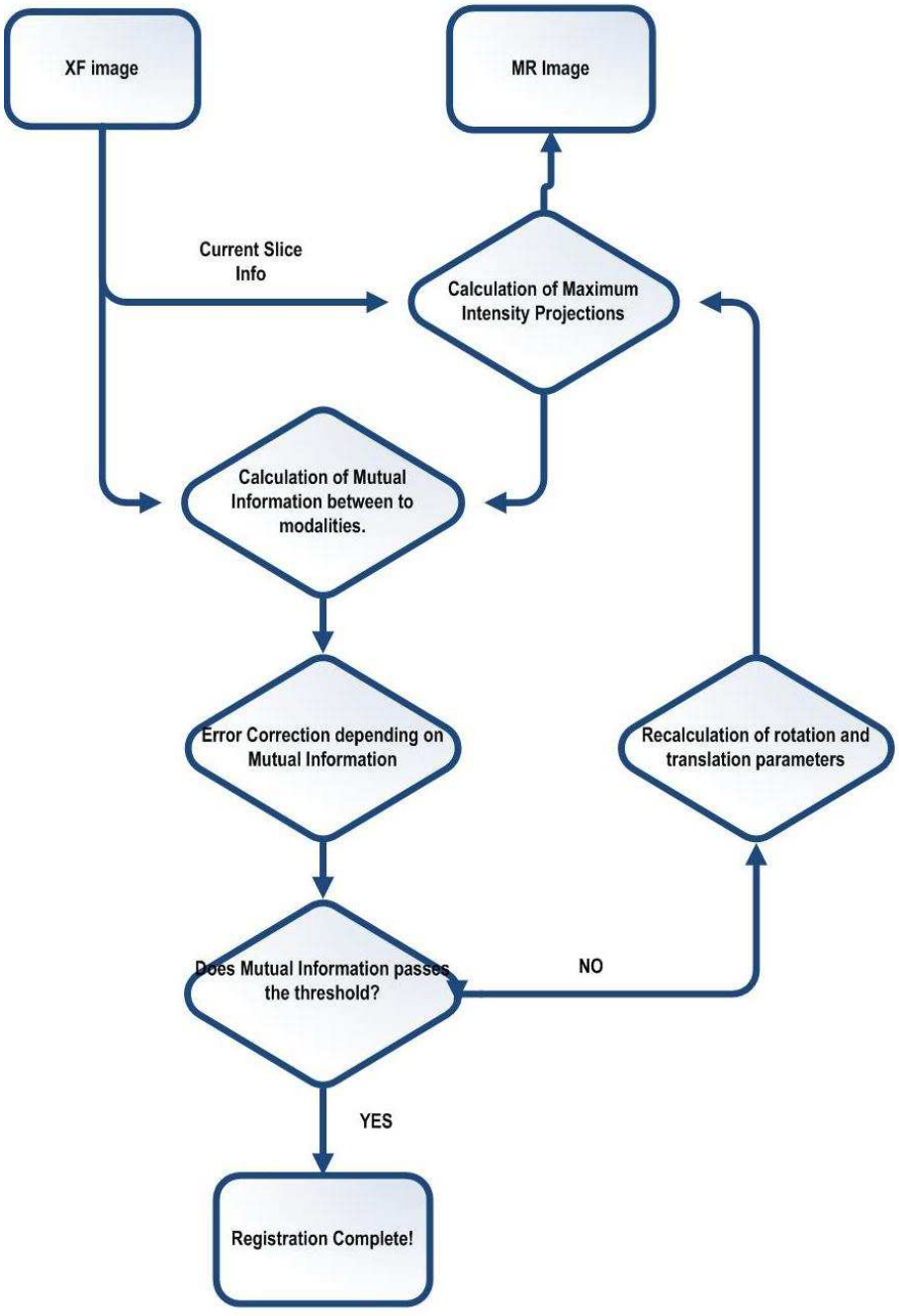

Figure 3.9 Optimization process for Registraiton Parameters. We are creating projection images of MRI by using the information from AX. Then we calculate the mutual information between two modalities, update our projection parameters iteratively and get registration result.

4. Results

Our aim is to register 3D MR Volume to 2D XF images by using image intensity informations. Here we compare our registration results with the results of the fiducial based registration method on 5 data sets. These in vivo data sets were taken during XFM procedures in animal experiments performed at NHLBI (National Heart Lung Blood Institute) part of NIH (National Institutes of Health), Bethesda, Maryland, US.

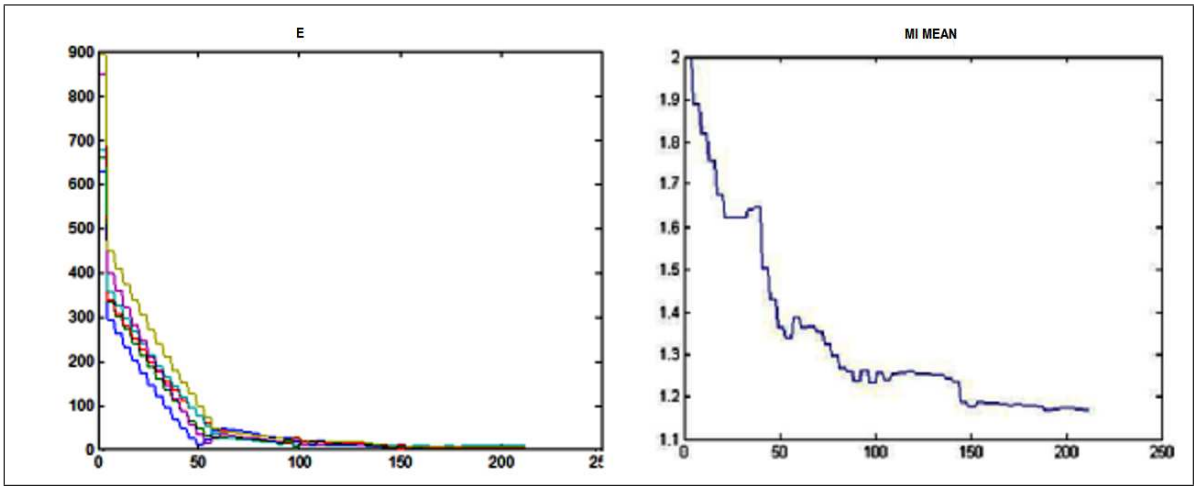

Figure 4.1 A comparison of error parameters during optimization. Left graph displays the distance between markers on fiducial registration method, error parameter changes with iterations. Right graph shows us the avarage mutual information error parameter evolution with iterations.

Intensity-based registration algorithm was tested on several situations. We have used the animal experiment data taken from NIH [38]. We calculate registration parameters according to least square minimization algorithm and compare results. Least square minimization helps us to minimize the error parameters for each unknown and get us the closest result. It is basically a curve fitting algorithm which finds the optimum values for this purpose. In our algorithm 3 translation, and 3 rotation parameters are unknowns. By using mutual information parameter and least square minimization algorithm we are able to find optimum values for this 6 unknowns.

Testing is made with a reverse problem. First we took the finalized projection data, and transform it over the 3-D space. We use predefined values to create a rotated and translated image from the final registered image. Then by using the intensity based

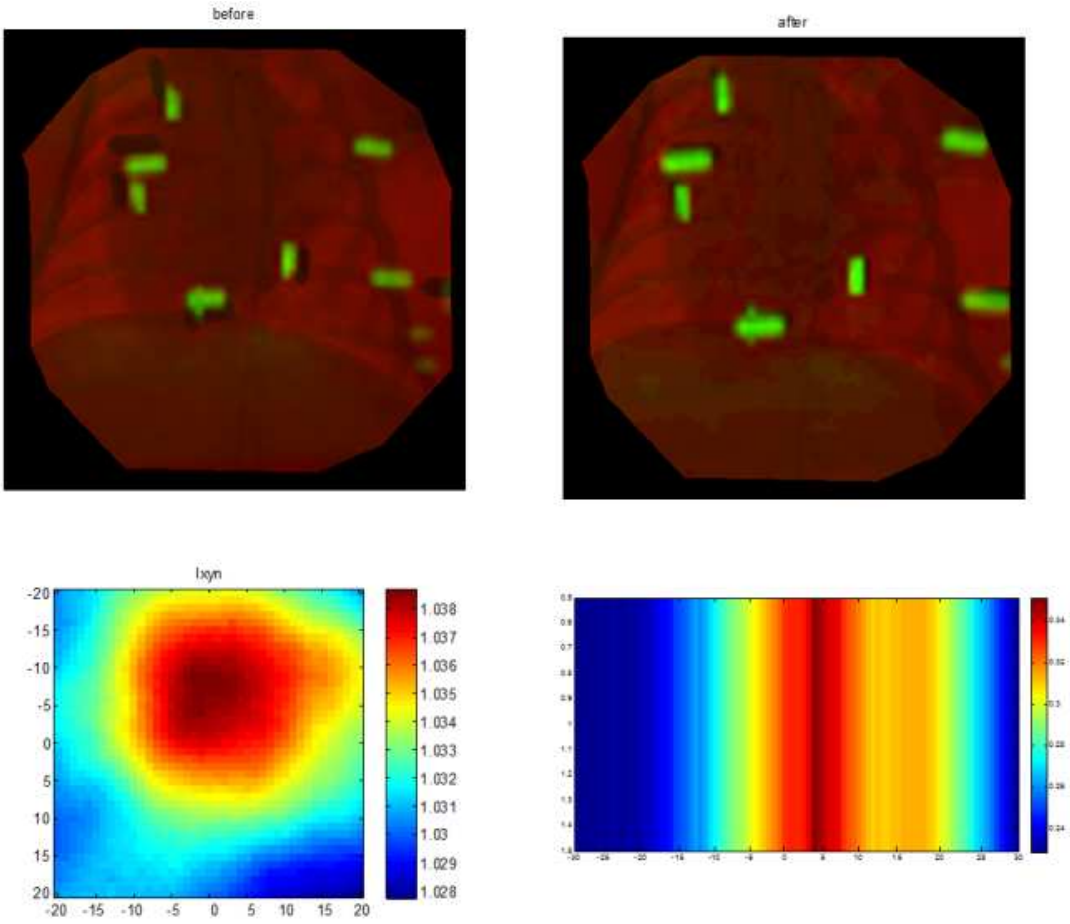

Figure 4.2 Comparison of Rigid Registration with Original Image Error is -7 px on y axis 2 px on x axis and -3^{o} rotation. Matching error is calculated with pixel by pixel mutual information comparison. For calculate matching error two images intensity pixel values are compared pixel by pixel and find the maximum match by translating, and rotating the image according to the reference image.

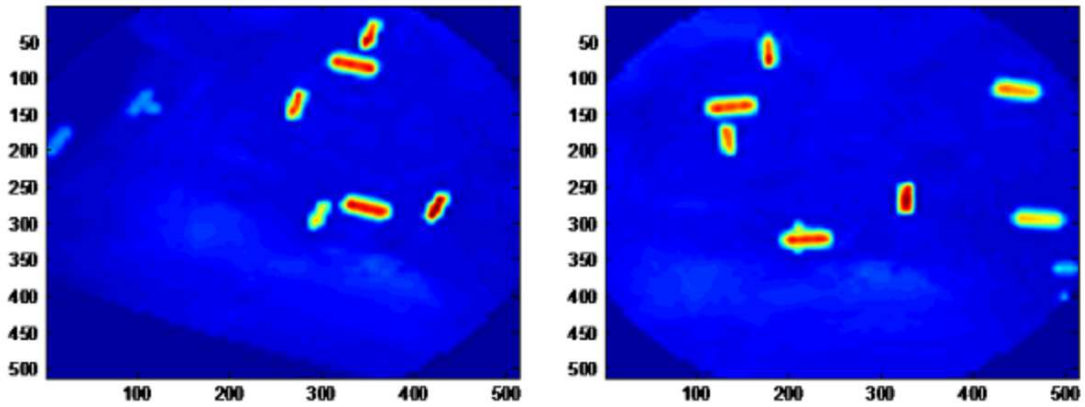

Figure 4.3 Left hand side is the manipulated MR projection. Our parameters are 30^{o} rotation on 3 dimensions. Translation on x axis is 50 pixels, translation on y axis is 20 pixels, and translation on z axis is 20 pixels. Right hand side is the result projection after intensity based registration. Registration time is 4107 seconds. First we translate the projection image with given parameters and check the time for registration process completes.

registration algorithm we find our initial position. According to tests registration takes between 300 seconds to 7000 seconds according to the distance from original registration parameters (Table 4.1) .

Our algorithm starts from initial start with approximated translation and rotation parameters. By iterative recalculation of parameters maximum intensity projection of the MR volume is creating and by calculating mutual information error parameter we are recalculating the rotation and translation parameters again. This process continues until mutual information error parameter is sufficient enough which show us a total registration occurs between two modalities.

We have used many different math calculations through the registration process. We have smoothed the mutual information error parameter through the time as in Figure 4.5 , we divide images into sub images to get more accurate results and less iterations, and we use least square minimization algorithm for optimization of our process. All these steps helps us to overcome the problems that we have meet during the intensity based registration process. Our main goal for this project was to make best accurate registration as fast as possible.

	Translation (x,y,z)	Rotation (x,y,z)	Time	Error (x)	Error (y)
UNIT:	pixel	pixel	(s)	mm	mm
simulation-1	0, 0, 0	20° ,20° ,20°	589	2.4	0.8
simulation-2	0,20,20	30°,30°,30°	1643	0.8	1.6
simulation-3	50,20,20	30°,30°,30°	4107	3.2	0.8
simulation-4	20,0,20	20°,0°,0°	357	0.8	0
simulation-5	20,0,20	0°,20°,0°	361	0	1.6
simulation-6	20,0,20	0°,0°,20°	348	0	0.8
simulation-7	50,30,40	20°,20°,20°	4929	1,6	2.4
simulation-8	100,30,40	20°,0°,0°	6833	0.8	0
simulation-9	100,40,60	0°,20°,0°	5366	0.8	0.8
simulation-10	150,40,60	0°,30°,0°	6527	0.8	1,6

Table 4.1
Experimental results on Registration. Different preassumptions are used for registration. We take the registered image and shift the image on space with certain translation and rotation parameters, than check the time and accuracy for registration. Error parameter is calculated by a different algorithm which is comparing the intensity of the results pixel by pixel.

Our results shows us even on cardiac procedures we can use intensity based registration algorithm on practice.

For the comparison between point-based registration and intensity based registration we compared error parameters of both algorithms. Automatic based registration depends on to calculate the distance between two identical markers on two different modalities which is explained in detail on section 2.1.1[38], intensity based registration error parameter is depends on the similarity of intensity values between two images. Distance, and mutual error parameters have a similar path. This path lead us to solve intensity based registration problem on XFM. Although automatic based registration can be faster on registration process it's pre-registration process, and absolute dependency on markers are two main problems. We take the distance error parameters for each markers position on X-ray and MRI, and compare this data with our mutual information based error parameter. In Figure 4.1 we show the two graphs one depends on fiducial based registration, and the other on intensity based algorithm.

After the registration process we have checked the overall registration success with comparing MR and X-ray images pixel by pixel. We take our registered images and check that on each point are the pixel values are identical or not, Figure 4.2 shows the comparison and error graphs, and Table 4.1 shows the experimental results on registration.

For testing our algorithm, first we translate and rotate the registered image on computer with certain values, and check that if registration occurs or not. Table 4.1 shows our algorithms respons on certain values to translation, and rotation value changes. In Figure 4.3 we rotate and translate the registered image with certain parameters (30^{0} rotation on 3 dimensions. Translation on x axis is 50 pixels, translation on y axis is 20 pixels, and translation on z axis is 20 pixels). Then we start registration process; registration took 4107 seconds from our predefined starting point. So for testing first we translate and rotate the projection image with given parameters and check the time for registration process completes.

Computer results shows that overall performance of our additions and XFM in general seems satisfactory for many clinical studies.

4.1 Mutual Information Error Parameters: Failures

Intensity based MR to X-ray registration is a difficult registration problem. MR is visualizing mainly soft tissues, on the other hand X-ray is good at visualizing bone structure and vessels with contrast. Because of this difference we had to be creative in this registration process. As we explain on chapter 3.3 one of the hardest problem is to find a starting point for registration. We first try to randomize the translation parameters and find a good start on space. However iterating images on 3D space without a pre-knowledge takes a lot of time, and most of the time, no match was found between the images.

During our optimization trials we try many different algorithms to reduce the processing time and get better results. We have 5 basic variables during this process. These are downsampling ratio, mutual information division on images, weight calculation for error parameter, local maximums and minimums, and initial registration parameters.

We try different down sampling ratios between 1-bit to 128-bit, we also down sample the XF image by using gaussian pyramid reconstruction, and resize it. Down sampling interval changes from 1-bit to 16-bit. Our results shows us the optimum result for registration is 8-bit quantized projection image with original X-ray image. If we downsample the MR image more than 8-bit we lose too much intensity data. On the other hand if we down sample the image less than 8-bit during optimization process our error parameter run into many local minimums and maximums which make our calculations impossible. For XF images other than downsampling and resizing takes time; we cannot observe any advantage of it (Figure 4.4).

During error parameters calculation on the optimization process there are many

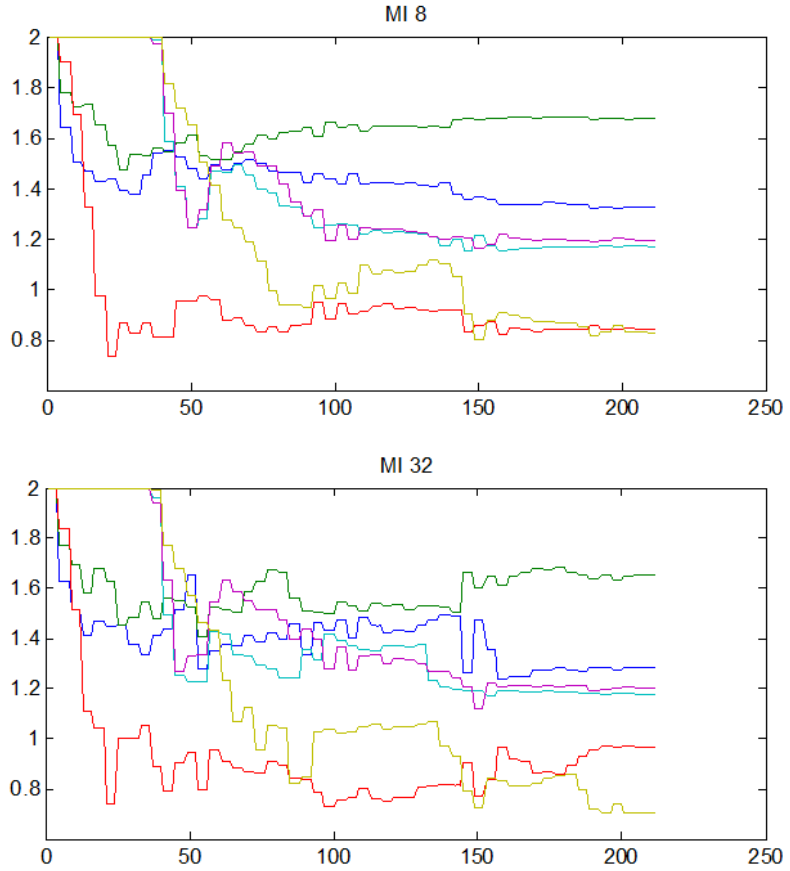

Figure 4.4 Difference of MI changing depending on the downsampling ratio. Upper-side graph has a downsampling ratio of 8, and lower-side graph has a downsampling ratio of 32. More downsampling causes lack of intensity information on the image, on the other hand less downsampling creates a very detailed intensity map on the image which causes failure in our algorithm. Due to presence of many local minima we optimise downsampling at 8 bit level provided best results.

dramatic local changes. These changes cause local minimums and maximums on the graph, which cause problems because process registration process depends on images which are continuously getting close to each other which means continuous decreasing on the curve. If the curve is not decreasing it means that images are not getting closer to registration, so algorithm makes a wrong approximation. To get rid of this problem we add a correction to our algorithm. If there is a unexpected increase on our mutual information error parameter we are skipping the registration parameters causing to this result and make a new iteration with new parameters (Figure 4.5).

In each step with better parameter assumptions images are getting close to registration. After a several hundred iterations images on both modalities are registered.

We take maximum intensity projections on each image calculate the mutual information error metric and iterate the images for better results with translation and rotation parameters (Figure 4.6).

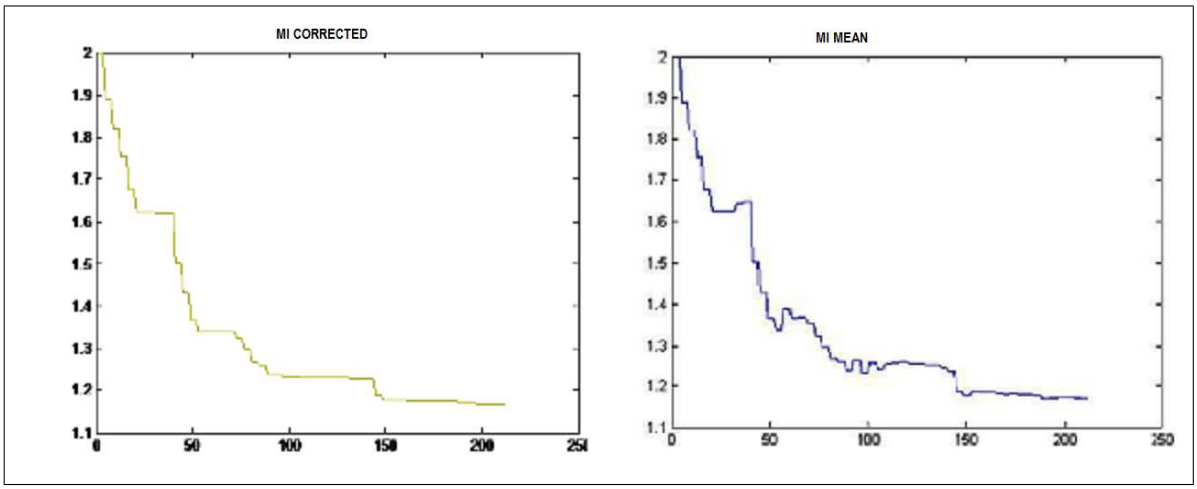

Figure 4.5 Correction of Mutual Information for get rid of local minima and maxima on the curve. Dramatic local changes cause mistakes on registration process so if a local maxima or minima occurs we generate different translation parameters for a better result. If there is a unexpected increase on our mutual information error parameter we are skipping the registration parameters causing to this result and make a new iteration with new parameters. This helps us to register faster and more accurate.

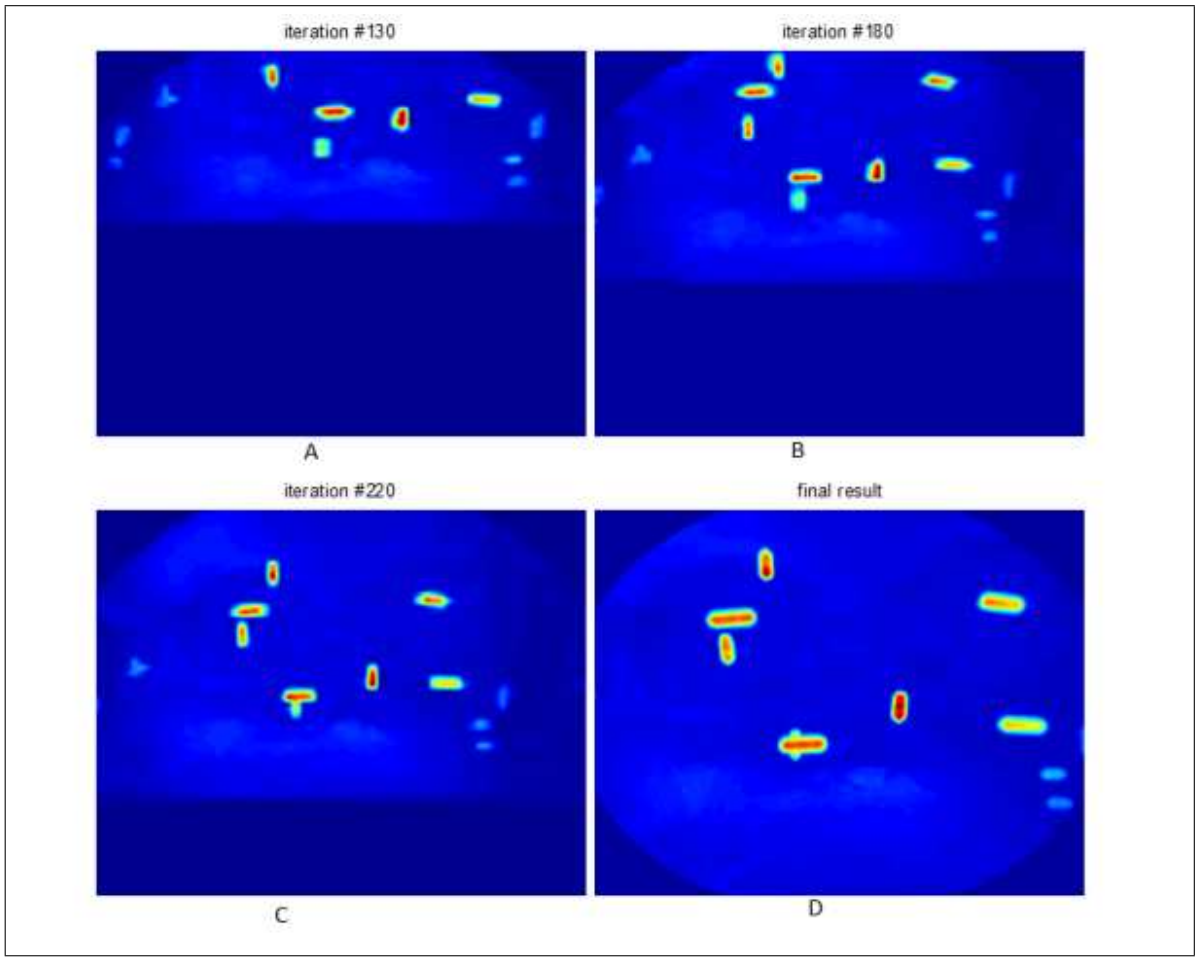

Figure 4.6 Changing of the MIP image during iterations. In each iteration better registration parameters calculates. A) Projection image after 130 iterations B) Projection image after 180 iterations C) Projection image after 220 iterations D) Projection image after final iteration. More iteration on the process helps us to get better results on registration through 3D space. Total iteration number for this example was around 300.

5. Future Work

X-ray Fused with MRI (XFM) is a tool for cardiovascular interventions. Main drawback of the current X-ray guided procedures is the lack of soft tissue contrast on X-ray.

Future work of this study should try to make a better optimization process to shorten the registration time. If we are able to make an accurate guess for initial starting point we will shorten the overall time and decrease the dependency on other algorithms. In our tests we saw that inital start for this configuration could be 10 pixels for Tx 400 pixels for Ty ,and 10 pixels for Tz. We also observe that rotation does not have a significant role. Algorithm needed to be tested further in-vivo experiments to see the true performance in clinical applications.

Never MR imaging techniques, ultrashort TE sequences, could be used to provide higher contrast of bone structure which could be used for mutual information with X-ray images in the future. X-ray imaging has essentially a bone imaging modality, having similar MR contrast as UTE (ultrashort TE sequence) would be very helpful.

As described in Section 1.2 many medical image registration methods exist, and each has its own strength and weakness, in the future we could combine two or more registration algorithms in a better way. For example we could employ an hybrid algorithm which combines intensity based registration with a feature-based algorithm. Certain features, like edges, on visible on both modalities can be segmented before registration and intensity based registration could be used guided solely by the reliable preprocessed image, or both data sets.

Here we have shown that if we have a fast and reliable algorithm for initial course registration of our algorithm has the potential to be fully automatic. For this purpose acquisition procedure could be updated and we could use the positioning information

coming from AX more effectively.

REFERENCES

1. E. Atalar, P.A. Bottomley, O. Ocali, L.C.L. Correia, M.D. Kelemen, J.A.C. Lima, and E.A. Zerhouni. High resolution intravascular MRI and MRS by using a catheter receiver coil. *Magnetic Resonance in Medicine*, 36(4):596–605, 1996.

2. E. Atalar, D.L. Kraitchman, B. Carkhuff, J. Lesho, O. Ocali, M. Solaiyappan, M.A. Guttman, and HK Charles. Catheter-tracking FOV MR fluoroscopy. *Magnetic Resonance in Medicine*, 40:865–872, 1998.

3. CJ Bakker, RM Hoogeveen, WF Hurtak, JJ Van Vaals, MA Viergever, and WP Mali. MR-guided endovascular interventions: susceptibility-based catheter and near-real-time imaging technique. *Radiology*, 202(1):273, 1997.

4. R. Bitar, G. Leung, R. Perng, S. Tadros, A.R. Moody, J. Sarrazin, C. McGregor, M. Christakis, S. Symons, A. Nelson, et al. MR Pulse Sequences: What Every Radiologist Wants to Know but Is Afraid to Ask1. *Radiographics*, 26(2):513, 2006.

5. A. Buecker, J.M. Neuerburg, G.B. Adam, A. Glowinski, T. Schaeffter, V. Rasche, J.J. van Vaals, A. Mølgaard-Nielsen, and R.W. Guenther. Real-time MR fluoroscopy for MR-guided iliac artery stent placement. *Journal of Magnetic Resonance Imaging*, 12(4):616–622, 2000.

6. A. Can, C.V. Stewart, B. Roysam, and H.L. Tanenbaum. A feature-based, robust, hierarchical algorithm for registering pairs of images of the curved human retina. *IEEE Transactions on Pattern Analysis and Machine Intelligence*, pages 347–364, 2002.

7. M.S. Cohen, R. Turner, H.M. Cheng, T.J. Brady, and B.R. Rosen. Dynamic magnetic resonance imaging of human brain activity during primary sensory stimulation. In *Proc. Nadl. Acad. Sci. USA*, volume 89, pages 5675–5679. National Acad Sciences, 1992.

8. E. Cosman. *Rigid Registration of MR and Biplanar*. PhD thesis, Massachusetts Institute of Technology, 2000.

9. J.R. Adler Jr. D.B. Russakoff, T. Rohlfing and C.R. Maurer Jr. Intensity based 2D-3D spine image registration incorporating a single fiducial marker. *Acad Radiology*, 12(1):37–50, 2005.

10. M. Ebara, Y. Murayama, T. Saguchi, T. Ishibashi, K. Irie, H. Takao, S. Sadaoka, E. Klotz, and T. Abe. Balloon Test Occlusion with Perfusion CT Imaging Utilizing Intraarterial Contrast Injection. *Interventional Neuroradiology*, 12(1):241–245, 2006.

11. R. Fahrig, K. Butts, J.A. Rowlands, R. Saunders, J. Stanton, G.M. Stevens, B.L. Daniel, Z. Wen, D.L. Ergun, and N.J. Pelc. A truly hybrid interventional MR/X-ray system: feasibility demonstration. *Journal of Magnetic Resonance Imaging*, 13(2):294–300, 2001.

12. R. Fahrig, G. Heit, Z. Wen, BL Daniel, K. Butts, and NJ Pelc. First use of a truly-hybrid X-ray/MR imaging system for guidance of brain biopsy. *Acta Neurochirurgica*, 145(11):995–997, 2003.

13. D. Gianfelice, L. Lepanto, P. Perreault, C. Chartrand-Lefebvre, and P.C. Milette. Value of CT fluoroscopy for percutaneous biopsy procedures. *Journal of Vascular and Interventional Radiology*, 11(7):879–884, 2000.

14. F. Godart, J.P. Beregi, L. Nicol, B. Occelli, A. Vincentelli, V. Daanen, C. Rey, and J. Rousseau. MR-guided balloon angioplasty of stenosed aorta: in vivo evaluation using near-standard instruments and a passive tracking technique. *Journal of Magnetic Resonance Imaging*, 12(4):639–644, 2000.

15. L.F. Gutierrez. *X-ray fused with MRI (XFM) for guidance of catheter-based interventions*. PhD thesis, Johns Hopkins University, 2006.

16. L.F. Gutierrez, C. Ozturk, E.R. McVeigh, and R.J. Lederman. Sparsely sampled distortion correction for a c-arm mounted x-ray image intensifier. *Medical physics*, 35:997, 2007.

17. L.F. Gutierrez, G. Shechter, R.J. Lederman, E.R. McVeigh, and C. Ozturk. Fiducial based registration of MR and X-ray images for MRI-guided catheter interven-

tions. In *Proceedings of the fifth interventional MRI symposium, Cambridge, MA*, 2004.

18. P. Heckbert. Color image quantization for frame buffer display. *ACM Siggraph Computer Graphics*, 16(3):297–307, 1982.

19. T. Jansson. Feature Based Registration. *Phys. Med. Biol.*, 2006.

20. D. Jones, DA Christopherson, JT Washington, MD Hafermann, JW Rieke, JJ Travaglini, and SS Vermeulen. A frameless method for stereotactic radiotherapy. *British Journal of Radiology*, 66(792):1142, 1993.

21. J. Jovicich, S. Czanner, D. Greve, E. Haley, A. van der Kouwe, R. Gollub, D. Kennedy, F. Schmitt, G. Brown, J. MacFall, et al. Reliability in multi-site structural MRI studies: effects of gradient non-linearity correction on phantom and human data. *Neuroimage*, 30(2):436–443, 2006.

22. V. Kapoor, B.M. McCook, and F.S. Torok. An Introduction to PET-CT Imaging1. *Radiographics*, 24(2):523, 2004.

23. T. Kuehne, M. Saeed, C.B. Higgins, K. Gleason, G.A. Krombach, O.M. Weber, A.J. Martin, D. Turner, D. Teitel, and P. Moore. Endovascular Stents in Pulmonary Valve and Artery in Swine: Feasibility Study of MR Imaging–guided Deployment and Postinterventional Assessment1. *Radiology*, 226(2):475, 2003.

24. E.M. Law, A.F. Little, and J.C. Salanitri. Non-vascular intervention with real-time CT fluoroscopy. *Australasian Radiology*, 45(2):109–112, 2001.

25. J.L. Leong, P.S. Batra, and M.J. Citardi. CT-MR image fusion for the management of skull base lesions. *Otolaryngology-Head and Neck Surgery*, 134(5):868–876, 2006.

26. JB Maintz and M.A. Viergever. A survey of medical image registration. *Medical image analysis*, 2(1):1–36, 1998.

27. C.R. Maurer Jr, J.M. Fitzpatrick, M.Y. Wang, R.L. Galloway Jr, R.J. Maciunas, and G.S. Allen. Registration of head volume images using implantable fiducial markers. *IEEE Transactions on Medical Imaging*, 16(4):447–462, 1997.

28. E.R. McVeigh, M.A. Guttman, R.J. Lederman, M. Li, O. Kocaturk, T. Hunt, S. Kozlov, and K.A. Horvath. Real-time interactive MRI-guided cardiac surgery: aortic valve replacement using a direct apical approach. *Magnetic resonance in medicine: official journal of the Society of Magnetic Resonance in Medicine/Society of Magnetic Resonance in Medicine*, 56(5):958, 2006.

29. O. Ocali and E. Atalar. Intravascular magnetic resonance imaging using a loopless catheter antenna. *Magnetic Resonance in Medicine*, 37(1):112–118, 1997.

30. R.A. Omary, R. Frayne, O. Unal, T. Warner, F.R. Korosec, C.A. Mistretta, C.M. Strother, and T.M. Grist. MR-guided angioplasty of renal artery stenosis in a pig model: a feasibility study. *Journal of Vascular and Interventional Radiology*, 11(3):373–381, 2000.

31. E.K. Paulson, D.H. Sheafor, D.S. Enterline, H.P. McAdams, and T.T. Yoshizumi. CT Fluoroscopy-guided Interventional Procedures: Techniques and Radiation Dose to Radiologists1. *Radiology*, 220(1):161, 2001.

32. G.P. Penney, J. Weese, J.A. Little, P. Desmedt, D.L.G. Hill, D.J. Hawkes, et al. A comparison of similarity measures for use in 2-D-3-D medical image registration. *IEEE Transactions on Medical Imaging*, 17(4):586–595, 1998.

33. K.S. Rhode, D.L.G. Hill, P.J. Edwards, J. Hipwell, D. Rueckert, G. Sanchez-Ortiz, S. Hegde, V. Rahunathan, and R. Razavi. Registration and tracking to integrate X-ray and MR images in an XMR facility. *IEEE Transactions on Medical Imaging*, 22(11):1369–1378, 2003.

34. K.S. Rhode, M. Sermesant, S. Hegde, G. Sanchez-Ortiz, D. Rueckert, R. Razavi, and D.L.G. Hill. XMR guided cardiac electrophysiology study and radio frequency ablation. In *Proc. SPIE, Medical Imaging*, volume 5369, pages 10–21, 2004.

35. T. Rohlfing and C. Maurer. A novel image similarity measure for registration of 3-D MR images and x-ray projection images. *Medical Image Computing and Computer-Assisted Intervention MICCAI 2002*, pages 469–476, 2002.

36. Y. Sato, N. Shiraga, S. Nakajima, S. Tamura, and R. Kikinis. Local maximum intensity projection (LMIP): a new rendering method for vascular visualization. *Journal of Computer Assisted Tomography*, 22(6):912, 1998.

37. S.G. Silverman, K. Tuncali, D.F. Adams, R.D. Nawfel, K.H. Zou, and P.F. Judy. CT Fluoroscopy-guided Abdominal Interventions: Techniques, Results, and Radiation Exposure1. *Radiology*, 212(3):673, 1999.

38. Merdim Sonmez. A Fiducial-Based Automatic Registration Method for X-ray Imaging Fused with MRI. Master's thesis, Bogazici University, Istanbul,Turkey, February 2008.

39. E. Spuentrup, A. Ruebben, T. Schaeffter, W.J. Manning, R.W. Gunther, and A. Buecker. Magnetic resonance-guided coronary artery stent placement in a swine model. *Circulation*, 105(7):874, 2002.

40. C.M. Strother. AXIOM Artis FD systems and DynaCT with AXIOM Artis FD systems and DynaCT it is possible to ACT providing soft tissue imaging in the angio suite. *AXIOM Innova tion in Intervention*, 1:12–13, 2005.

41. R.H. Taylor, BD Mitterlstadt, H.A. Paul, et al. An image-directed robotic system for precise orthopedic surgery. *Computer-Integrated Surgery, Technology and Clinical Applications*, pages 379–396.

42. D. Tomazevic, B. Likar, T. Slivnik, and F. Pernus. 3-D/2-D registration of CT and MR to X-ray images. *IEEE Transactions on Medical Imaging*, 22(11):1407–1416, 2003.

43. I. Vajda. *Theory of Statistical Inference and Information*. Kluwer Academic Pub, 1989.

44. R.L. Wahl, L.E. Quint, R.D. Cieslak, A.M. Aisen, R.A. Koeppe, and C.R. Meyer. " Anatometabolic" Tumor Imaging: Fusion of FDG PET with CT or MRI to Localize Foci of Increased Activity. *Journal of Nuclear Medicine*, 34(7):1190, 1993.

45. W. Wein. Intensity based rigid 2D-3D registration algorithms for radiation therapy. *Technische Universitat MÃ¼nchen, Diplomarbeit*, pages 15–27, 2003.

46. W. Wein, B. Roper, and N. Navab. Automatic registration and fusion of ultrasound with CT for radiotherapy. *Lecture Notes in Computer Science*, 3750:303, 2005.

47. C.S. White, C.A. Meyer, and P.A. Templeton. CT fluoroscopy for thoracic interventional procedures. *Radiologic Clinics of North America*, 38(2):303–322, 2000.

48. K. Yonetsu, M. Sumi, M. Izumi, M. Ohki, S. Eida, and T. Nakamura. Contribution of Doppler sonography blood flow information to the diagnosis of metastatic cervical nodes in patients with head and neck cancer: assessment in relation to anatomic levels of the neck. *American Journal of Neuroradiology*, 22(1):163, 2001.

49. B. Zitova and J. Flusser. Image registration methods: a survey. *Image and vision computing*, 21(11):977–1000, 2003.

50. L. Zollei. 2D-3D rigid-body registration of X-ray fluoroscopy and CT images. Master's thesis, Massachusetts Institute of Technology, Boston,USA, 2001.